GOF = 2.155; Δ/σ(mean) = 0.00; highest peak in difference map = 1.17 e/Å^3 (all peaks larger than 1.0 e/Å^3 were ghosts of the tungsten atom).

Acknowledgment. We thank the National Science Foundation (Grant CHE-8814729) for support of this work. Support for T.K.S. was provided by the Department of Education under the GAANN program. The Deutscher Akademischer Austauschdienst provided support for A.W. We also thank Professor Steven George, David Haynes, and Kathleen Helwig for their assistance with the lifetime measurements.

Supplementary Material Available: Tables of bond distances and angles, hydrogen atom coordinates, and thermal parameters (4 pages); table of observed and calculated structure factors (9 pages). Ordering information is given on any current masthead page.

Photophysical Studies in Solution of the Tetranuclear Copper(I) Clusters $Cu_4I_4L_4$ (L = Pyridine or Substituted Pyridine)[1-3]

Kevin R. Kyle, Chong Kul Ryu, John A. DiBenedetto, and Peter C. Ford*

Contribution from the Department of Chemistry, University of California, Santa Barbara, California 93106. *Received October 3, 1990. Revised Manuscript Received December 5, 1990*

Abstract: Reported are the emission and excitation spectra and emission lifetimes of a series of tetranuclear copper(I) clusters of the type $Cu_4I_4L_4$ (L = pyridine, substituted pyridine, or a saturated amine) in solution and in the solid state. These materials are bright, relatively long-lived emitters in room-temperature solution which display two emission bands, an intense lower energy (LE) band (λ_{max} = 690 nm, $\tau_{(LE)}$ = 11.1 μs for $Cu_4I_4(py)_4$, I, in 293 K toluene), and a much less intense higher energy (HE) band (λ_{max} = 480 nm, $\tau_{(LE)}$ = 0.45 μs for I, in 293 K toluene). Comparisons of substituent and solvent effects as well as the observation that this band is not seen for L = saturated amine have led to the conclusion that the HE emissiion is from an excited state either metal-to-ligand charge transfer (MLCT) or iodide-to-ligand charge transfer (XLCT) in character. The LE band is assigned as emission from a cluster-centered (CC) excited state, possibly an iodide-to-metal charge transfer. The two emissions show different excitation spectra as well as different lifetime and relative intensity profiles as the temperature is lowered. At lower T (e.g., 77 K), the emission spectra of the well-characterized solids display properties similar to the solutions of the same compounds in frozen solutions. The rates of selective quenching of the HE excited state by Lewis bases as well as by energy transfer (at room temperature) are reported as are the quenching rates of both states by O_2. The independent behavior of the lifetimes and excitation spectra of the HE and LE emissions for various $Cu_4I_4L_4$ all indicate that the excited states responsible are essentially uncoupled.

Introduction

There has been considerable recent interest in the photophysical properties of mononuclear and polynuclear complexes of transition metals in oxidation states having the d^{10} electronic configuration.[3-13] Among these, the tetranuclear clusters of copper(I) display remarkably rich photoluminescence properties.[3,9-13] One particularly notable example is the pyridine cluster $Cu_4I_4(py)_4$ (I), which has been shown by X-ray crystallographic analysis[14] to have a tetrahedral structure, such as A. The Cu-Cu distances in this structure are quite short (2.69 Å in I),[14] although, to a first approximation, there is no formal covalent metal-metal bonding between these ground-state d^{10} metal centers. This structure and others of analogous $Cu_4I_4L_4$ clusters can be viewed as tetrahedra of copper centers with the tetrahedral faces capped by iodides comprising a larger tetrahedron (I-I distances of 4.50 Å in I[14] and ligands L coordinated at the apices of the Cu_4 tetrahedron). For simplicity, clusters having this configuration will be referred to as being the "cubane" isomers to distinguish them from those having a "staristep" configuration as illustrated by B.

With the exception of several recent reports[3,12,13] including preliminary communications of the present work, photophysical properties of the tetranuclear copper(I) clusters have been largely concerned with studies in the solid state. Among earlier studies, Hardt and co-workers[9] showed that emission maxima of pyridine adducts of cuprous halides when excited in the UV are markedly temperature-dependent for solids of stoichiometry CuIL. This phenomenon was termed *luminescence thermochromism*. These studies were largely phenomenological, reporting syntheses, lu-

(1) Taken in part from the Ph.D. Dissertation of K. R. Kyle, UC Santa Barbara, 1989.

(2) Presented in part at the 196th National Meeting of the American Chemical Society, Los Angeles, CA, September 1988 and at the Eighth International Symposium on the Photochemistry and Photophysics of Coordination Compounds, Santa Barbara, CA, August 1989.

(3) Preliminary communications describing this work in part: (a) Kyle, K. R.; DiBenedetto, J. A.; Ford, P. C. *J. Chem. Soc., Chem. Commun.* **1989**, 714-715. (b) Kyle, K. R.; Ford, P. C. *J. Am. Chem. Soc.* **1989**, *111*, 5005-5006.

(4) (a) Crosby, G. A.; Highland, R. G.; Truesdell, K. A. *Coord. Chem. Rev.* **1985**, *64*, 41-53. (b) Kutal, C. *Coord. Chem. Rev.* **1990**, *99*, 213-252.

(5) (a) Caspar, J. V. *J. Am. Chem. Soc.* **1985**, *107*, 6718-6719. (b) Harvey, P. D.; Gray, H. B. *J. Am. Chem. Soc.* **1988**, *110*, 2145-2147.

(6) (a) Balch, A. L.; Nagle, J. K.; Oram, D. E.; Reedy, P. E., Jr. *J. Am. Chem. Soc.* **1988**, *110*, 454-462. (b) King, C.; Wang, J.-C.; Khan, M. N. I.; Fackler, J. P., Jr. *Inorg. Chem.* **1989**, *28*, 2145-2149.

(7) (a) McMillin, D. R.; Kirchhoff, J. R.; Goodwin, K. V. *Coord. Chem. Rev.* **1985**, *64*, 83-92. (b) Ichinaga, A. K.; Kirchhoff, J. R.; McMillin, D. R.; Dietrich-Buchecker, C. O.; Marnot, P. A.; Sauvage, J.-P. *Inorg. Chem.* **1987**, *26*, 4290-4292. (c) Crane, D. R.; DiBenedetto, J.; Palmer, C. E. A.; McMillin, D.; Ford, P. C. *Inorg. Chem.* **1988**, *27*, 3698-3700. (d) Parker, W. L.; Crosby, G. A. *J. Phys. Chem.* **1989**, *93*, 5692-5696. (e) Casandonte, D. J.; McMillin, D. R. *J. Am. Chem. Soc.* **1987**, *109*, 331-337.

(8) Stillman, M. J.; Zelazowski, A. J.; Szynmanska, J.; Gasyna, Z. *Inorg. Chim. Acta* **1989**, *161*, 275-279.

(9) (a) De Ahna, H. D.; Hardt, H. D. *Z. Anorg. Allg. Chem.* **1972**, *387*, 61-71. (b) Hardt, H. D.; Gechnizdjani, H. *Z. Anorg. Allg. Chem.* **1973**, *397*, 23-30. (c) Hardt, H. D.; Pierre, A. *Z. Anorg. Allg. Chem.* **1973**, *402*, 107-117. (d) Hardt, H. D. *Naturwissenschaften* **1974**, *61*, 107-110. (e) Hardt, H. D.; Pierre, A. *Inorg. Chim. Acta* **1977**, *25*, L59-L60. (f) Hardt, H. D.; Pierre, A. *Annal. Univer. Saraviensis* **1980**, *15*, 7-28. (g) Hardt, H. D.; Stoll, H.-J. *Z. Anorg. Allg. Chem.* **1981**, *480*, 193-198. (h) Hardt, H. D.; Stoll, H.-J. *Z. Anorg. Allg. Chem.* **1981**, *480*, 199-204.

(10) (a) Radjaipour, M.; Oelkrug, D. *Ber. Bunsenges. Phys. Chem.* **1978**, *82*, 159-163. (b) Eitel, E.; Oelkrug, D.; Hiller, W.; Strahle, J. *Z. Naturforsch.* **1980**, *35b*, 1247-1253.

(11) (a) Rath, N. P.; Holt, E. M.; Tanimura, K. *Inorg. Chem.* **1985**, *24*, 3934-3938. (b) Rath, N. P. Ph.D. Dissertation, Oklahoma State University, 1985. (c) Rath, N. P.; Holt, E. M.; Tanimura, K. *J. Chem. Soc., Dalton Trans.* **1986**, 2303-2310. (d) Rath, N. P.; Maxwell, J. L.; Holt, E. M. *J. Chem. Soc., Dalton Trans.* **1986**, 2449-2453. (e) Tompkins, J. A.; Maxwell, J. L.; Holt, E. M. *Inorg. Chim. Acta* **1987**, *127*, 1-7.

(12) Vogler, A.; Kunkely, H. *J. Am. Chem. Soc.* **1986**, *108*, 7211-7212.

(13) Henary, M.; Zink, J. I. *J. Am. Chem. Soc.* **1989**, *111*, 7407-7411.

(14) Raston, C. L.; White, A. H. *J. Chem. Soc., Dalton Trans.* **1976**, 2153-2156.

0002-7863/91/1513-2954$02.50/0

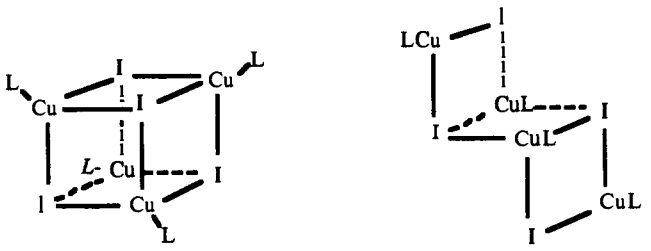

A B

minescence maxima, and color and temperature dependences, although various explanations were offered for the luminescence thermochromism.

Oelkrug and co-workers have studied the solid-state emission dynamics of the $Cu_4I_4(py)_4$ cluster.[10] They demonstrated the existence of two emissive states; a higher energy emission (λ_{max} 435 nm) was the dominant feature at low temperature, while a lower energy emission (585 nm) was dominant at higher temperatures. The observed emission behavior also included dependence on the excitation wavelength (λ^{ex}) at low temperature. The natures of the emissive states were not unambiguously assigned, although it was argued that a cubane structure appeared to be a necessary condition for luminescence thermochromism.

Holt and co-workers[11] have correlated crystal structural properties with the emission characteristics of several cuprous iodide aromatic amine complexes. They concluded that metal–metal interactions are crucial to the emission behavior and noted that the lower energy emission is displayed only by those clusters with copper–copper internuclear distances <2.8 Å. The polymeric species $[CuIpy]_\infty$, which has a stairstep type of structure and exhibits only a higher energy emission, has a Cu–Cu distance of 2.875 Å. These data suggested that the cluster longer wavelength emission derives from a metal-centered phenomenon that involves more than one metal center.[11a]

The photoluminescence of the copper(I) tetramers in solution has remained relatively unexplored. Hardt observed that solutions of I in benzene exhibited a red luminescence and attributed this behavior to spontaneous decomposition to form highly dispersed cuprous iodide which undergoes emission from lattice defects.[9c] This interpretatioin was contested by results obtained by Vogler and Kunkely, who demonstrated by osmometry that $Cu_4I_4(py)_4$ and $Cu_4I_4(morpholine)_4$ remain intact in benzene solution.[12] Both complexes exhibited a broad red emission band in benzene at room temperature for which the respective emission maxima λ_{max} (698 nm and 654 nm), τ_{em} (900 ns and 300 ns), and Φ_{em} (0.04 and 0.004) were reported. The observation that both the morpholine (saturated amine) and the pyridine (aromatic amine) complexes displayed similar luminescence behavior precluded the assignment of the emissive state as MLCT in nature, and these data were interpreted as being indicative of a $3d^{10} \rightarrow 3d^94s^1$ copper-centered excited state.

Henary and Zink[13] have recently described the emission properties of an analogous tetranuclear copper(I) chloride cluster ($Cu_4Cl_4(DENC)_4$ (DENC = *N,N*-diethylnicotinamide)) and of related mixed-metal tetranuclear complexes in low-temperature methylene chloride glasses. Again a red emission band was observed for each of these complexes (even when the ligand field states of the heterometal center were at lower energy), and these workers concluded that this photophysical property was the result of emission from a Cu(I) localized $3d^94s^1$ excited state strongly modified by copper–copper interactions.

Our interest in the photophysical properties of the polynuclear Cu(I) complexes was originally drawn by the dramatic Stokes shifts between the high energies of the absorption bands of these white (or sometimes pale yellow) compounds and the low energies of the red emission bands. It was further stimulated by the concept that a 3d → 4s transition should be (formally) an antibonding to bonding transition, which should lead to enhanced metal–metal bonding in these $3d^{10}$ (ground state) clusters in analogy to the now extensively investigated d^8–d^8 dimers[15] such as the platinum(II) anion $Pt_2(\mu\text{-}P_2O_5H_2)_4^{4-}$, which have shown considerable promise in photocatalysis applications.[15b] In this article we describe the solution spectroscopy and photoluminescence lifetimes of a collection of tetranuclear clusters $Cu_4I_4L_4$ (L = an aromatic or saturated amine in most cases) and some related complexes of different nuclearities. In addition are discussed some results involving bimolecular energy transfer of these clusters. As will be noted these polynuclear complexes display remarkably rich photophysical properties, which can only be attributed to the poor coupling between various excited states of different orbital parentages.

Experimental Section

Materials. Gases were purchased from Linde. Nitrogen and argon were either used as received, or, when used with the high vacuum manifold (HVM), were deoxygenated by passing the gas through a column of BASF copper Deox catalyst and then a silica gel supported chromous column. Solvents were prepared as follows. Benzene and toluene (Burdick and Jackson High Purity solvent) were dried over CaH_2 and distilled under nitrogen. Isooctane (Aldrich Gold label) was washed successively with H_2SO_4, H_2O, $NaHCO_3$(aq), and finally H_2O, dried over $MgSO_4$, and distilled from CaH_2 under argon. Tetrahydrofuran was distilled from sodium benzophenone ketal under nitrogen. Chlorobenzene, 2,5-dimethyltetrahydrofuran (DMTHF), methyl acetate, hexanes, and methanol were distilled from CaH_2 under nitrogen. Methylene chloride was distilled from $LiAlH_4$ under nitrogen. Deuterated benzene, C_6D_6, was vacuum distilled from $LiAlD_4$ prior to use. Water was deionized and then distilled in an all-glass apparatus from weakly basic $KMnO_4$ solution.

Copper(I) iodide (98%, Alfa Products) was purified by the method of Kauffmann[16] by dissolving in saturated aqueous KI, filtering, and then reprecipitating by addition of water to give an off-white powder. Pyridine and various pyridine derivatives were used as received or were purified as follows. Liquid amines were distilled from sodium metal or KOH pellets under nitrogen. Orange 4-phenylpyridine (99%, Aldrich) was recrystallized several times from hot hexanes to give white crystals. White needles of 2,6-diphenylpyridine (97%, Aldrich) were obtained via recrystallization from hot ethanol. Tri-*n*-butylphosphine was distilled and stored under argon.

Synthesis of the Metal Complexes. $Cu_4I_4(py\text{-}x)_4$. Pyridine and substituted pyridine adducts of copper(I) iodide were synthesized by the following general methods. (1) The simplest scheme is that of Malik.[17] An excess of ligand as a liquid or in acetone solution was added to a stirred solution of CuI in concentrated aqueous KI solution. The product, which precipitated immediately or upon standing a few minutes, was separated by filtration and then washed successively with saturated $KI_{(aq)}$ to remove excess CuI, H_2O to remove KI, methanol to remove excess ligand, and hexanes. Yields were quantitative based on the amount of copper used. The product was dried in vacuo and stored under nitrogen. (2) Another procedure is that outlined by Davies.[18] A stoichiometric amount of ligand as a liquid or in CH_2Cl_2 solution was added via syringe to a stirred suspension of CuI in dry CH_2Cl_2 under nitrogen. The suspension of CuI slowly dissolved, leaving a clear solution. After 1–6 h of stirring, a suspension of $Cu_4I_4L_4$ formed. Addition of hexanes facilitated precipitation. The product was recovered by filtration and washed as above. (3) A third procedure involved adding a stoichiometric amount of L to a stirred suspension of $[Cu(MeCN)_4]BF_4$ (prepared from Cu_2O and HBF_4 in acetonitrile)[19] and KI powder in dry benzene under nitrogen. The suspension of $[Cu(MeCN)_4]BF_4$ immediately cleared, and, after stirring 10 min, a precipitate of $Cu_4I_4L_4$ formed. The product was filtered and worked up as above. (4) This method was similar to (1) except that the product was extracted into CH_2Cl_2 and then precipitated by addition of hexanes. The advantage was 2-fold: aqueous impurities were left behind, and, in the cases where more than one product formed, the insoluble polymeric form ($[CuIL]_\infty$) was left behind, and only the soluble tetramer was extracted. (5) While some complexes could not be obtained by directly mixing CuI and the desired ligand, they were readily obtained by ligand metathesis with preformed $Cu_4I_4L_4$. This was exemplified by the reaction of 4-acetylpyridine with $Cu_4I_4(3\text{-}Clpy)_4$. An excess of 4-acetylpyridine (75 μL, 6.8×10^{-4} mol) was added to a stirred solution of $Cu_4I_4(3\text{-}Clpy)_4$ (92 mg, 7.6×10^{-5} mol) in benzene under

(15) (a) Zipp, A. P. *Coord. Chem. Rev.* **1988**, *84*, 47–83, and references therein. (b) Roundhill, D. M.; Gray, H. B.; Che, C. M. *Acc. Chem. Res.* **1989**, *22*, 55–61, and references therein.

(16) Kauffmann, G. B.; Teter, L. A. *Inorg. Synth.* **1963**, *7*, 9–12.

(17) Malik, A. U. *J. Inorg. Nucl. Chem.* **1967**, *29*, 2106–2107.

(18) Churchill, M. R.; Davies, G.; El-Sayed, M. A.; Hutchinson, J. P.; Rupich, M. W. *Inorg. Chem.* **1982**, *21*, 995–1001.

(19) Kubas, G. J. *Inorg. Synth.* **1979**, *19*, 90–92.

nitrogen. Hexanes were added to the resulting yellow-orange solution to deposit a yellow-orange microcrystalline solid. The product was washed with liberal amounts of methanol to remove excess ligand and then hexanes. The resulting yellow powder was shown to be free of 3-Clpy by comparing the product IR spectrum with that of an authentic sample of $Cu_4I_4(3\text{-Cl-py})_4$.

The tetrameric clusters were recrystallized by stirring in benzene or toluene to give a saturated solution. In some cases, activated charcoal was added to decolorize the solution. After filtering through fluted filter paper, hexanes were added to precipitate the product as a powder. Alternatively, hexanes were added up to the point where precipitation just begins. The mixture was then cooled in the freezer, giving crystals. The products were washed with methanol and then hexanes and finally dried under vacuum. They were stored under nitrogen, usually in the freezer. The crystalline solid of $Cu_4I_4py_4$ was characterized by comparing its powder X-ray diffraction pattern to the published values,[14] and a C/H/N elemental analysis in good agreement with the formulation $Cu_4I_4(Phpy)_4$ was obtained for the 4-phenylpyridine complex. The other tetranuclear py-x derivatives were assumed to have the tetranuclear formulation owing to the analogous synthetic procedures used to obtain crystalline products and the strong correlation between their photophysical properties.

It should be noted that the solvent used for recrystallization can modify the form of the copper complex obtained.[20,21] For example, recrystallization of $Cu_4I_4(PPh_3)_4$ from $CHCl_3$ has been shown to give a "step" tetramer.[22] The same complex was obtained as the familiar "cubane" polymorph when recrystallized from toluene.[20] Similar behavior was noted for I. When recrystallized from benzene, toluene, or CH_2Cl_2, prismatic crystals of the tetramer were obtained. Recrystallization from a benzene/methanol mixture resulted in a mixture of $[CuI(py)]_\infty$ and the tetramer.

$[CuI(py)]_\infty$. This was synthesized via two methods. The first, the method of Eitel et al.,[10b] involved the addition of CuI and pyridine in stoichiometric amounts to acetonitrile at 60 °C. After 2 days, needles of $[CuI(py)]_\infty$ formed. The second method involved the addition of a stoichiometric amount of pyridine to a solution of CuI dissolved in a saturated KI solution of 1/1 H_2O/MeOH at 40 °C. The step polymer precipitated immediately and was worked up as outlined above for the cubane form.

$Cu_4I_4(P(n\text{-}Bu)_3)_4$. This was prepared according to the published procedure.[16] The complex was recrystallized from 1/1 EtOH/*i*-PrOH, and stored under nitrogen in the freezer.

$Cu_4I_4L_4$ (L = Piperidine or Morpholine). The saturated amine tetranuclear complexes were prepared by literature procedures[23] or by the first procedure described above for the synthesis of I.[17] The CHN analysis (Galbraith Laboratories Inc.) of the piperidine complex was in agreement with the formulation $Cu_4I_4(pip)_4$. Anal. Calcd for $C_{20}H_{40}N_4Cu_4I_4$: C, 21.79; H, 4.02; N, 5.08. Found: C, 21.70; H, 4.13; N, 5.02.

$Cu_2I_2(Et_4en))_2$ (Et_4en = *N,N,N',N'*-Tetraethylethylenediamine). The dimeric complex of the saturated amine Et_4en was prepared by the published procedure.[24] The product was obtained as a white powder after filtering and washing under nitrogen. It was dried in vacuo and stored under nitrogen.

$Cu_2I_2(py)_4$. (Di-μ^2-iodo)tetrakis(pyridine)dicopper(I) was prepared by a modification of the published procedure.[25] Copper(I) iodide was dissolved in neat pyridine, yielding a yellow solution. Addition of a 10-fold excess of hexanes resulted in the formation of yellow microcrystals. These were washed once with hexanes. The complex was stored under pyridine-saturated nitrogen. The dinuclear compound proved to be unstable relative to the tetramer $Cu_4I_4(py)_4$. Washing with methanol gave only the cubane cluster, as did allowing pyridine to evaporate from the dimer.

Instrumentation. IR spectra were measured with a Digilab FTS-60 spectrophotometer. Electronic absorption spectra were recorded with a Cary 118C (1-cm cell or 1.75-cm diameter quartz fluorimetry tube) or an HP 8452A diode array (1-cm cell) spectrophotometer. Proton (^1H) NMR spectra were obtained on a General Electric 500-MHz NMR spectrometer operating in a pulsed FT mode with deuterium lock. The X-ray diffraction pattern of $Cu_4I_4(py)_4$ was obtained by Dr. Mike Eddy of UCSB by using a Blake Industries four-circle diffractometer interfaced to a DEC VAX II computer.

Luminescence Spectra and Lifetime Procedures. Solutions for emission studies were prepared by using the HVM or a conventional Schlenk vacuum/gas manifold. Sample preparation on the HVM involved degassing and drying of a solvent via 3–5 freeze–pump–thaw cycles over Na/K mirror, followed by vacuum distillation onto the sample. Sample preparation on the Schlenk line involved distillation of the solvent under nitrogen prior to use, followed by deaeration by bubbling with nitrogen. Solvent was then introduced to the sample cell via syringe under positive nitrogen pressure. Sample solutions for emission lifetime and spectra measurements were prepared in a four window quartz 1-cm fluorescence cell or a 1.75-cm diameter quartz fluorimetry tube. Both cells were equipped with greaseless Rotoflo stopcocks for anaerobic use. Samples were typically 10^{-4}–10^{-5} M in dry, deaerated solvent under N_2 or Ar. Temperature control for lifetime measurements was maintained with a Haake FK circulating refrigerated and heated water bath at 294 ± 0.5 K. Variable-temperature emission lifetime and spectra measurements of solution samples were performed by using the 1.75-cm fluorimetry cell. The temperature was maintained in a quartz optical dewar with the appropriate bath: 294 (H_2O), 273 (ice/H_2O), 250 (CO_2/CCl_4), 231 (CO_2/MeCN), 195 (CO_2/acetone), 77 K (liquid N_2).[26] Solid samples were prepared as powders in quartz capillary tubes under nitrogen. Limited studies of the solid samples were carried out with an Oxford Instrument variable-temperature cryostat.

Luminescence lifetime measurements were made on two different instrumental systems.[27] The first employed an AVCO ERL C-950 pulsed nitrogen gas laser as the excitation source (λ_{ex} = 337 nm). Emission was monitored at a right angle to the excitation beam. The emitted light was passed through a Fastie–Ebert 0.8 m scanning grating monochromator and then an O-52 Corning glass or KV-389 Schott plastic filter to remove laser scatter and was detected by an RCA 8852 PMT operating at 800–1200 V. The PMT output was monitored with a Princeton Applied Research 4400 boxcar averager with a 4422 gated integrator and 4402 signal processor. Data were collected at a single wavelength and stored as PMT output vs time in Waveform mode (scanning time gate). A Pacific Photoinstruments Model 50 phototube provided the trigger pulse for the boxcar.

The second system for lifetime measurements utilized a Quanta Ray DCR-1A Q-switched Nd/YAG pulsed laser operating at 10 Hz as the excitation source. The system was equipped with an HG-1 harmonic generator and a PHS-1 harmonic separator to isolate the desired third harmonic (355 nm). The output power at 355 nm was typically 12 mJ/pulse. Specific wavelength dichroic mirrors mounted on beam steering towers were used to direct the excitation beam and to ensure laser line quality at the sample. The sample emission was monitored at a right angle to the excitation source. The sample emission was filtered (KV-389) to reduce laser scatter prior to entering a SPEX Model 1680 Doublemate grating monochromator blazed at 500 nm. The emission intensity was monitored at selected wavelengths with an RCA 8852 or EMI 9816A fast response PMT. The PMT output was terminated (50 Ω) into a Tektronix 7912AD transient digitizer equipped with a Tek 7B90P programmable timebase and a 7A13 differential comparator amplifier. The system response time has been measured with DCM laser dye in MeOH, giving a laser pulse width (FWHM) of 14 ns and a response time of 6 ns. The signal averaged data (average of 64 shots per 512 point array) were processed with a Tektronix 4052 graphic display microcomputer or a Zenith ZF-158-42 PC. Data were analyzed by a least-squares fit of ln (intensity) vs time or by exponential curve fitting.

Emission and excitation spectra were recorded utilizing a SPEX Fluorolog 2 spectrophotometer equipped with a Hamamatsu R928A water cooled PMT configured for photon counting and interfaced with a SPEX Datamate II data station. Emission spectra were corrected for phototube response. Excitation spectra were corrected for lamp intensity variation by the ratio method with a Rhodamine 6G reference.

Emission quantum yields were determined on the SPEX spectrophotometer by using the modified Parker–Rees method[28,29] with $Ru(bpy)_3^{2+}$ in deaerated water (0.042) as the quantum yield reference.[30] Integrated emission intensities were corrected for background and PMT response.

(20) Dyason, J. C.; Healy, P. C.; Englehardt, L. M.; Pakawatchai, C.; Patrick, V. A.; Raston, C. L.; White, A. H. *J. Chem. Soc., Dalton Trans.* **1985**, 831–838.
(21) Toth, A.; Floriani, C.; Chiesi-Villa, A.; Guastina, C. *Inorg. Chem.* **1987**, *26*, 3897–3902.
(22) Churchill, M. R.; DeBoer, B. G.; Donovan, D. J. *Inorg. Chem.* **1975**, *14*, 617–623.
(23) (a) Schramm, V. *Inorg. Chem.* **1978**, *17*, 714–718. (b) Schramm, V.; Fischer, K. F. *Naturwissenschaften* **1974**, *61*, 500–501.
(24) Churchill, M. R.; Davies, G.; El-Sayed, M. A.; Fournier, J. A.; Hutchinson, J. P.; Zubieta, J. A. *Inorg. Chem.* **1984**, *23*, 783–787.
(25) Dyason, J. C.; Engelhardt, L. M.; Healy, P. C.; White, A. H. *Aust. J. Chem.* **1984**, *37*, 2201–2205.
(26) Gordon, A. J.; Ford, R. A. *The Chemists Companion*; John Wiley & Sons: New York, 1972; p 451.
(27) (a) Weber, W.; van Eldik, R.; Kelm, H.; DiBenedetto, J.; Ducommun, Y.; Offen, H.; Ford, P. C. *Inorg. Chem.* **1983**, *22*, 623–628. (b) DiBenedetto, J. A. Ph.D. Dissertation, UC Santa Barbara, 1985.
(28) Bergkamp, M. A.; Brannon, J.; Magde, D.; Watts, R. J.; Ford, P. C. *Chem. Phys. Lett.* **1978**, *59*, 125–128.
(29) Demas, J. N.; Crosby, G. A. *J. Phys. Chem.* **1971**, *75*, 991–1024.
(30) Van Houten, J.; Watts, R. J. *J. Am. Chem. Soc.* **1976**, *98*, 4853–4858.

Time-Resolved Emission Spectra. These were obtained by using the PAR 4400 system described above. The Fastie–Ebert 0.8 m monochromator was scanned at a rate of 50 nm/min. With a laser pulse rate of 30 Hz, the output of the boxcar averager represented the average of at least 25 intensity measurements for each 1-nm segment of the spectrum. Traces of PMT output vs wavelength were collected in Static Gate mode. Data were collected for a short time gate (2–50 ns in duration) after the boxcar was triggered. Time resolution of the spectra was the result of a variable delay time. Data stored on disk by the PAR 4402 data station were converted to ASYST/ASYSTANT format by a program written by Christine Miller. Time-resolved spectra were uncorrected for phototube response.

Emission Quenching. Emission lifetimes of $Cu_4I_4(py)_4$ at 298 K were measured in the presence and absence of various quenchers with the Nd/YAG laser system. Solutions were prepared by using a modification of the transfer bulb described by Wink[31] (which provided a closed system under nitrogen) by serial addition of aliquots (5–100 μL) of a quencher stock solution to a solution of I (10^{-5}–10^{-4} M, 10–20 mL) inside the transfer bulb under positive nitrogen pressure and were deaerated before use. Solutions for self-quenching studies were prepared by serial dilution of a stock solution of I (initially 10^{-3}–10^{-2} M) with deaerated solvent. Solutions for oxygen-quenching studies were prepared by bubbling with O_2 for >10 min.

Data obtained at different quencher concentrations were treated by Stern–Volmer kinetics.[32] Bimolecular quenching constants, k_q, were calculated from the slope, K_{SV}, according to $k_q = K_{SV}/\tau_0$, where τ_0 is the lifetime in the absence of quencher. Self-quenching data were plotted as τ^{-1} vs [I], giving the intercept τ_0^{-1} and slope k_q which were determined by linear least-squares analysis with the program LSQUARES on a Hewlett Packard 87XM computer.

Results

A. Characteristics of $Cu_4I_4(py)_4$ (I) and Related Species. Physical Properties. The majority of the tetrameric clusters $Cu_4I_4L_4$ were obtained as white powders or as colorless crystals, although when L is a ligand with extended π conjugation, e.g., 4-phenylpyridine, the recrystallized solids proved to be pale yellow in color. The $Cu_4I_4(py)_4$ prepared in this laboratory displayed the solid-state and benzene solution emission spectra described previously,[9e,10b,12] and the X-ray powder diffraction study gave crystal cell parameters identical with those reported for the single-crystal structure.[14] The solubility of I in benzene, acetone, and CH_2Cl_2[12] was confirmed, and solubility in toluene, chlorobenzene, methyl ethyl ketone, methyl acetate, 2-methoxyethanol, 2-methoxyethyl ether, THF, and DMTHF was demonstrated. In contrast, polymeric forms such as $[CuIpy]_\infty$ proved to be insoluble in the aforementioned solvents. The structures of the other py-x adducts of CuI described herein were inferred to be analogous to I by the similarities of their emission characteristics and solubilities. Notably, a number of other $Cu_4I_4L_4$ complexes, including those where L = morpholine[23a] or piperidine,[23b] have been characterized by X-ray crystallography to have a structure analogous to A.[33]

Given the labilities of Cu(I) complexes to ligand substitution reactions (see below), one must be concerned that in solution the tetranuclear complexes may undergo fragmentation to species of lower nuclearities. The tetranuclear complexes "self-assemble" from their constituents under a variety of synthetic conditions (see Experimental), and Vogler[12] and Davies[18] have utilized molecular weight determinations to demonstrate that the $Cu_4I_4L_4$ clusters maintain their integrity in solution. In the present study, this conclusion was supported by linear Beer's law plots, as exemplified by Figure 1, consistent with a single species or a collection of species of identical composition being present in solution. The observed thermal stability of I relative to dimeric and polymeric

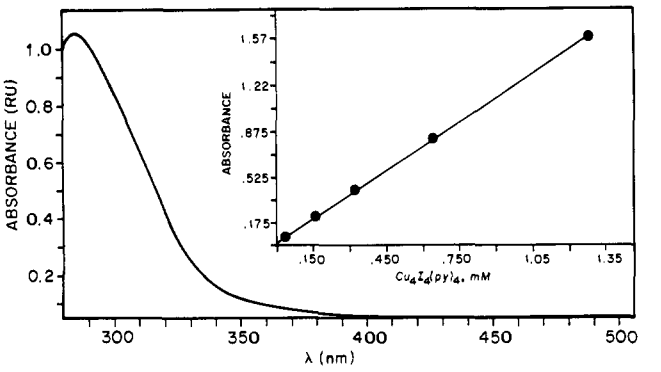

Figure 1. (a) Beer's law plot: abs (360 nm) vs $[Cu_4I_4(py)_4]$ in benzene solution. (b) UV spectrum of $Cu_4I_4(py)_4$ in benzene at 25 °C.

copper(I) species also supports the contention that $Cu_4I_4(py)_4$ retains its tetrameric form in solution. For example, it was observed that $Cu_2I_2(py)_4$ spontaneously associates to I upon dissolving in benzene (as monitored by emission spectroscopy). Washing $Cu_2I_2py_4$ with methanol also resulted in the immediate formation of I. Furthermore, the polymeric form $[CuIpy]_\infty$ irreversibly converted to $Cu_4I_4(py)_4$ upon heating in the solid state.

The IR spectra of the $Cu_4I_4(py\text{-}x)_4$ complexes (KBr pellets) are dominated by the pyridine vibrational transitions only slightly perturbed upon complexation to Cu(I). The Cu_4I_4 core vibrations of I have been reported to lie in the far-IR (138, 87 cm^{-1}).[34]

NMR Spectra. The ^1H NMR spectrum of $Cu_4I_4(py)_4$ in C_6D_6 consists of three sets of resonances due to the ortho (H_a, doublet, δ 9.23 ppm), meta (H_b, triplet of triplets, δ 6.75 ppm), and para (H_c, triplet, 6.51 ppm) protons in an integrated ratio 2/2/1. The splitting pattern is analogous to that of free pyridine but with H_a appearing at lower field (deshielded) by 0.69 ppm and with H_b and H_c at higher field (shielded) by 0.27 and 0.20 ppm, respectively. Since coordination of py to a cationic center would be expected to have a deshielding effect on all ligand protons, the upfield shifts of H_b and H_c are suggestive of some π-backbonding interaction from Cu(I) into the py orbitals as argued previously for complexes of Ru(II) and low-spin Fe(II) as well of Cu(I) itself.[35] The NMR spectra of $Cu_4I_4(3\text{-}Clpy)_4$ and $Cu_4I_4(4\text{-}t\text{-}Bupy)_4$ gave similar observations.

When free py was added to C_6D_6 solutions of I, separate signals for free and coordinated pyridine were not observed; the H_a, H_b, and H_c resonances were the concentration weighted averages of those expected for $Cu_4I_4(py)_4$ and free py. Increasing [py] resulted in a further shift of the ^1H NMR peak positions toward the values for free py, the behavior being indicative of rapid exchange in solution between the free and coordinated pyridines. In the same context, addition of 4-*tert*-butylpyridine (tbpy) to a C_6D_6 solution of I resulted in the observation of single sets of proton resonances each for pyridine and for tbpy at frequencies intermediate between those characteristic of the free pyridines and coordinated pyridines. Again this result indicated that the exchange and redistribution between the coordinated and free ligand states (eq 1) is rapid on the time scale of the NMR experiment (>10^3 s^{-1}) and confirmed the marked lability of these d^{10} metal centers

$$Cu_4I_4(py)_4 + py\text{-}x = Cu_4I_4(py)_{4-n}(py\text{-}x)_n + npy \qquad (1)$$

where $Cu_4I_4(py)_{4-n}(py\text{-}x)_n$ represents a collection of mixed-ligand clusters with "*n*" ranging from 1 to 4.

Electronic Absorption Spectroscopy. No visible range absorption bands were observed in the solution-phase spectra of I or of the other $Cu_4I_4(py\text{-}x)_4$ clusters. The UV spectra are characterized by an onset of absorption about 400 nm with an increasing extinction coefficient extending to shorter wavelength. The main

(31) Wink, D. A. Ph.D. Dissertation, UC Santa Barbara, 1985.
(32) Turro, N. J. *Modern Molecular Photochemistry*; Benjamin/Cummings: Menlo Park, CA, 1978; pp 243–264.
(33) (a) Examples of $Cu_4I_4L_4$ complexes which have been shown by X-ray crystallography to have the "cubane"-type structure as in A include those where L = DENC,[18] piperidine,[23a] morpholine,[23b] 2-(diphenylmethyl)-pyridine,[33b] Et_3P,[33c] Et_3As,[33c] $(Me_2N)_3P$,[33d] and Ph_3P.[20] (b) Engelhardt, L. M.; Healy, P. C.; Kildea, J. D.; White, A. H. *Aust. J. Chem.* **1989**, *42*, 107–113. (c) Churchill, M. R.; Kalva, K. L. *Inorg. Chem.* **1974**, *13*, 1899–1904. (d) Arkhireeva, T. M.; Bulychev, B. M.; Sizov, A. I.; Sokolova, T. A.; Belsky, V. K.; Soloveichik, G. L. *Inorg. Chem. Acta* **1990**, *169*, 109–118.
(34) (a) Bowmaker, G. A.; Knappstein, R. J.; Tham, S. F. *Austr. J. Chem.* **1978**, *31*, 2137–2143. (b) Bowmaker, G. A.; Healy, P. C. *Spectrochim. Acta* **1988**, *44A*, 115–119.
(35) (a) Foust, R. D.; Ford, P. C. *J. Am. Chem. Soc.* **1972**, *94*, 5686–5696. (b) Marlin, J. M.; Schmidt, C. F.; Toma, H. E. *Inorg. Chem.* **1975**, *14*, 2924–2928. (c) Kitagawa, S.; Munkata, M.; Miyaji, N. *Inorg. Chem.* **1982**, *21*, 3842–3843.

Table I. Electronic Absorption Spectra of Some $Cu_4I_4(L)_4$ Complexes[a]

L	λ[b]	ε[c]
pyridine (in C_6H_6)	360 (sh)	740
	304 (sh)	3880
	284 (p)	12700
pyridine (in CH_2Cl_2)	360 (sh)	630
	290 (sh)	4180
	256 (p)	10800
pyridine (in THF)	360 (sh)	403
	306 (sh)	11320
	282 (p)	18110
4-phenylpyridine	360 (sh)	1150
	310 (sh)	6490
	292 (p)	11410
4-benzylpyridine	355 (sh)	1100
	309 (sh)	14700
	287 (p)	22400
4-*tert*-butylpyridine	360 (sh)	790
	306 (sh)	16200
	286 (p)	22900
3-chloropyridine	355 (sh)	140
	300 (sh)	2250
morpholine	355 (sh)	300
	305 (sh)	6900
	284 (p)	9700
piperidine	350 (sh)	1120
tri-*n*-butylphosphine	355 (sh)	650
	310 (sh)	7340
	286 (p)	11400

[a] In benzene solution (except where noted). [b] Wavelength in nm, sh = shoulder; p = peak. [c] Extinction coefficients in M^{-1} cm^{-1}.

features in benzene solution are a low-energy tail extending from 400 nm to about 340 nm, a shoulder at about 305 nm, and a peak around 290 nm. (It should be noted that the position of this maximum may be an artifact of the experimental conditions which mostly employed the solvent benzene which cuts off at $\lambda < 280$ nm.) The spectrum of I is shown in Figure 1 and absorption spectra characteristics of this cluster in benzene, CH_2Cl_2, and THF and of other $Cu_4I_4L_4$ complexes in benzene are listed in Table I.

The nature of the transitions giving rise to the UV absorption features is not immediately obvious from these data. Metal-centered (MC) or metal cluster core centered (MCC) transitions would be consistent with the observation of near-UV absorptions for $Cu_4I_4L_4$ clusters of both saturated and unsaturated amine ligands. Transitions which are metal-to-ligand charge transfer (MLCT) in nature might also be expected for π-unsaturated L's, such as aromatic amines; however, absorption spectra provide no convincing evidence in this regard. Such ligands would be expected to display ligand-centered (LC) $\pi-\pi^*$ transitions. The λ_{max} at 256 nm for I in CH_2Cl_2 would be consistent with the expected position of pyridine LC bands.

B. Emission Spectra. Spectra of Solid-State Materials. The solid-state luminescence spectrum of I at room temperature displays a single, broad structureless band centered at λ_{max} 580 nm with an excitation spectrum maximum at 380 nm (Figure 2), consistent with previous reports.[9d,10] Other $Cu_4I_4(py\text{-}x)_4$ tetramers

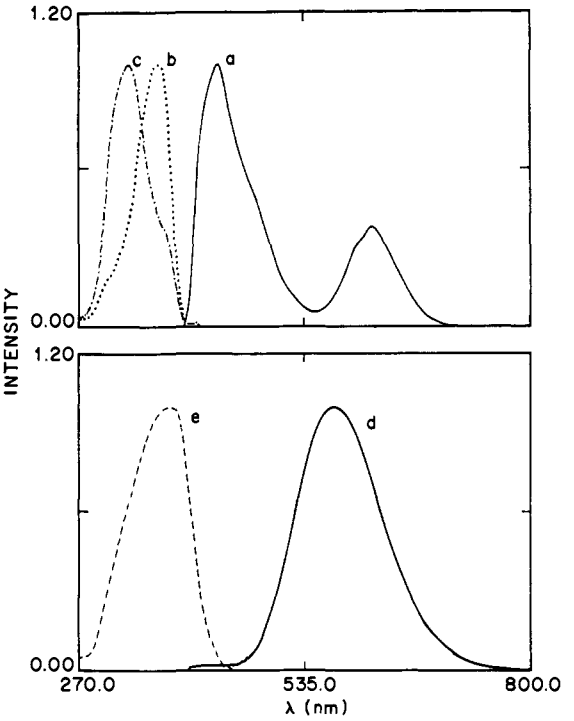

Figure 2. Emission and excitation spectra of solid $Cu_4I_4(py)_4$ at 294 K (lower) and at 77 K (upper): (a) emission spectrum (λ_{max} = 438 and 619 nm); (b) excitation spectrum monitoring at 438 nm (λ^{ex}_{max} = 365 nm); (c) excitation spectrum monitoring at 619 nm (λ^{ex}_{max} = 330 nm) (d) emission spectrum (λ_{max} = 580 nm); (e) excitation spectrum monitoring at 580 nm (λ^{ex}_{max} = 380 nm).

displayed analogous emission and excitation maxima as did the saturated amine cluster $Cu_4I_4(piperidine)_4$ (II). The pattern was different for the polymer $[CuIpy]_\infty$, which does not possess the tetrahedral Cu_4I_4 core and which displays an asymmetric emission band with a λ_{max} at 437 nm which tails to longer wavelength. The dimeric complex $Cu_2I_2(py)_4$ exhibits an emission band centered at 517 nm in the solid state. A similar emission band centered at 522 nm was seen for the saturated amine dimer complex $Cu_2I_2(Et_4en)_2$. These spectral properties are summarized in Table II.

Emission spectra at 77 K for various $Cu_4I_4(py\text{-}x)_4$ and related complexes are also summarized in Table II. Consistent with the earlier reports for I,[9,10] these each show two bands, a broad lower energy emission (LE) somewhat narrower and shifted to the red from that seen at 294 K and a new emission at much higher energy, e.g., see Figure 2. In contrast, the saturated amine complex II exhibits a single emission band centered at 590 nm. Thus, the presence of the new higher energy emission (HE) appears to depend on L being π-unsaturated. The dimeric complexes of $Cu_2I_2(Et_4en)_2$ and $Cu_2I_2(py)_4$ each exhibit a single emission band at 77 K. The energies of the emitting states were estimated as that point at which intensity drops to 1% of the λ_{max} intensity on the high-energy side of the band. If the emission has a Gaussian

Table II. Electronic Emission Maxima and Estimated E^{00} of $Cu_4I_4(py\text{-}x)_4$ and Related Complexes in the Solid State at 294 and at 77 K[a]

	294 K			77 K		
complex	λ_{max} ($\Delta\nu_{1/2}$)[b]	E^{00}[c]	λ^{ex}_{max}[d]	λ_{max} ($\Delta\nu_{1/2}$)[b]	E^{00}[c]	λ^{ex}_{max}[d]
$Cu_4I_4(py)_4$	580 (3.5)	21.8	380	619 (1.8)	18.5	330
				438 (3.1)	26.9	365
$Cu_4I_4(py\text{-}d_5)_4$	580 (3.5)	21.8		619 (1.8)	18.5	
				433 (3.0)	26.9	
$Cu_4I_4(tbpy)_4$	623 (3.3)	20.3		650 (1.9)	17.8	327
				437 (3.1)	26.9	362
$Cu_4I_4(pip)_4$	590 (3.4)	21.3		590 (2.0)	19.5	
$[CuIpy]_\infty$	437 (3.5)	27.4				
$Cu_2I_2(py)_4$	517 (4.7)	25.4		510 (4.5)	25.4	
$Cu_2I_2(Et_4en)_2$	522 (4.8)	25.3		544 (3.2)	22.5	

[a] λ^{ex} = 350 nm. [b] λ_{max} in nm; $\Delta\nu_{1/2}$ in kK (kK = 10^3 cm^{-1}). [c] E^{00} (kK) estimated as $E^{00} = \nu_{max} + 1.29\Delta\nu_{1/2}$. [d] λ_{max} for excitation band.

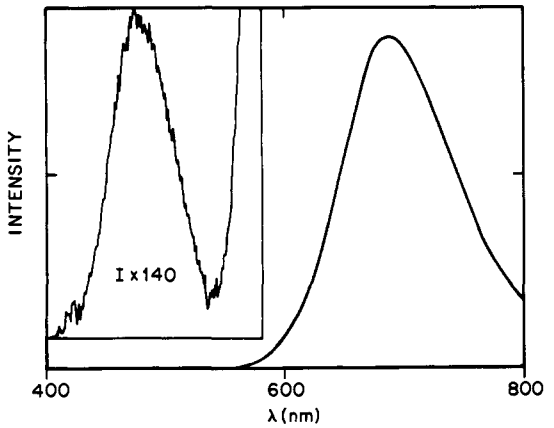

Figure 3. Emission spectrum of $Cu_4I_4(py)_4$ in 294 K toluene showing the weak HE emission band (inset).

Table III. Emission Spectral Data for Various $Cu_4I_4L_4$ in Toluene

		HE		LE	
L	T (K)	I_{max} ($\Delta\nu_{1/2}$)[a]	E^{00}[b]	λ_{max} ($\Delta\nu_{1/2}$)[a]	E^{00}[b]
4-*tert*-butylpyridine	294	468 (3.8)	26.3	696 (2.4)	17.5
	231	458 (4.3)	27.4	714 (2.3)	17.0
	195	450 (4.1)	27.5	727 (1.7)	16.0
	77	434 (3.7)	27.8	595 (2.9)	20.6
4-benzylpyridine	294	473[c] (3.9)	26.2	692 (2.4)	17.5
pyridine-d_5	294	480 (2.8)	24.5	690 (2.3)	17.5
	231	465 (4.1)	26.8	703 (2.2)	17.0
pyridine	294	480 (2.8)	24.5	690 (2.3)	17.5
	77	436 (4.0)	28.1	583 (2.2)	20.0
4-phenylpyridine	294	520 (3.1)	23.2	694 (2.3)	17.4
	250	512 (3.2)	23.6	698 (2.1)	17.0
	195	508 (3.6)	24.3		
	77	505 (3.7)	24.6		
3-chloropyridine	294	537[c] (2.3)	21.6	675 (2.5)	18.0
piperidine	294			680 (2.6)	18.1
morpholine	294			671 (2.6)	18.3
	77			630 (2.9)	19.6
P(*n*-Bu)$_3$	294			654 (2.8)	18.9
	77			620 (2.7)	19.6

[a] λ_{max} in nm; $\Delta\nu_{1/2}$ in kK. [b] E^{00} in kK, estimated according to text. [c] From time-resolved spectra.

band shape (intensity vs ν), this energy would be given by $E^{00} = \nu_{max} + 1.29\Delta\nu_{1/2}$, where $\Delta\nu_{1/2}$ is the full width at half maximum and ν_{max} is the band maximum (in kK).[36]

The excitation spectra for the solid aromatic amine complexes $Cu_4I_4(py\text{-}x)_4$ are quite temperature-dependent as illustrated in Figure 2 for $Cu_4I_4(py)_4$. Remarkably, at 77 K the LE emission band (λ_{max} 619 nm) for this complex displays an excitation maximum (λ^{ex}_{max}) at 330 nm, while the HE emission (λ_{max} 428 nm) displayed a λ^{ex}_{max} at 365 nm (Table II). This behavior clearly indicates thermally nonequilibrated excited states for the solid $Cu_4I_4(py\text{-}x)_4$ clusters at 77 K.

Emission Spectra in Solution. In ambient temperature toluene solution, both I and $Cu_4I_4(mor)_4$ were shown to display emission bands (λ^{ex} 350 nm) centered at 690 and 671 nm, respectively, the former being quite intense and in agreement with the report by Vogler[12] of such emissions in benzene solution. However, close examination of the emission spectrum of I revealed a second, much weaker HE band at 480 nm which had not been previously reported (Figure 3). The more intense LE band was the dominant feature of the emission spectrum for each of the tetranuclear $Cu_4I_4L_4$ clusters examined including several substituted pyridines as well as the saturated amines morpholine and piperidine and $(n\text{-Bu})_3P$; however, the weaker HE emission was exclusively a property of the aromatic amine complexes. The relevant spectral information is summarized in Table III. Notably, for L = py-x, the LE emission shows only a very modest sensitivity to the nature of the substituent, x, but the λ_{max} and calculated E^{00} values of the HE emission vary systematically with the more electron-donating pyridine substituents shifting the band to higher energy. The 294 K solution emission spectra of I in several different solvents showed the LE band to be essentially unaffected but the λ_{max} of the HE band to be fairly solvent sensitive (Table IV).

Table IV. Solvent Dependence of $Cu_4I_4(py)_4$ Emission Spectrum at 294 K

	HE		LE	
solvent	λ_{max}[a]	E^{00}[b]	λ_{max}[a]	E^{00}[b]
CH_2Cl_2	500 (sh)	~23.0	694	17.4
toluene	480	24.5	690	17.5
DMTHF	460	25.4	687	17.5
THF	465	25.9	689	17.5
methyl acetate	425[c]	27.9	693	17.5

[a] λ_{max} in nm. [b] E^{00} in kK, estimated according to text. [c] From time-resolved spectra.

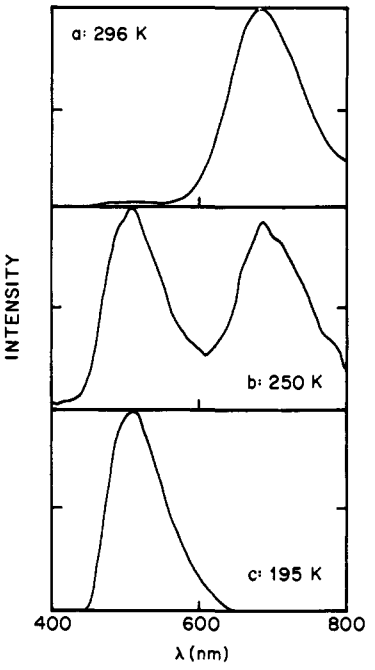

Figure 4. Temperature dependence of the emission spectrum of Cu_4I_4-(4-Phpy)$_4$ in toluene solution.

The fluid toluene solution emission spectra of the $Cu_4I_4(py\text{-}x)_4$ proved to be markedly temperature-dependent with the two bands shifting in different directions as well as changing in relative intensities. At lower temperature, the LE band was observed to red shift, while the HE band underwent a concomitant blue shift and became much brighter when the temperature was decreased to 195 K. These effects are summarized for several clusters in Table III and are illustrated for $Cu_4I_4(4\text{-Phpy})_4$ in Figure 4. Decrease of T to 77 K to give a rigid toluene glass leads to a further blue shift of the HE band but to a marked *blue* shift of the LE band in a direction reversing the pattern seen for the temperature effects in fluid solution. For I the λ_{max} of the LE band in frozen toluene is 583 nm, very close to the value seen for the solid (Table II). Since λ_{max} for the LE band is essentially independent of the solvent identity, this shift suggests the 77 K spectrum reflects a strong dependence upon the rigidity of the medium. This "rigidochromic effect"[37] is presumably responsible for the large red shifts the LE bands of the $Cu_4I_4(py\text{-}x)_4$ clusters experience in solution relative to the solid state. Vogler has shown that the LE λ_{max} for I in a room-temperature polymethylmethacrylate film has the intermediate value of 610 nm,[12] perhaps

(36) Peterson, J. D.; Watts, R. J.; Ford, P. C. *J. Am. Chem. Soc.* **1976**, *98*, 3188–3194.

(37) (a) Wrighton, M.; Morse, D. L. *J. Am. Chem. Soc.* **1974**, *96*, 998–1003. (b) Lees, A. J. *Chem. Rev.* **1987**, *87*, 711–743.

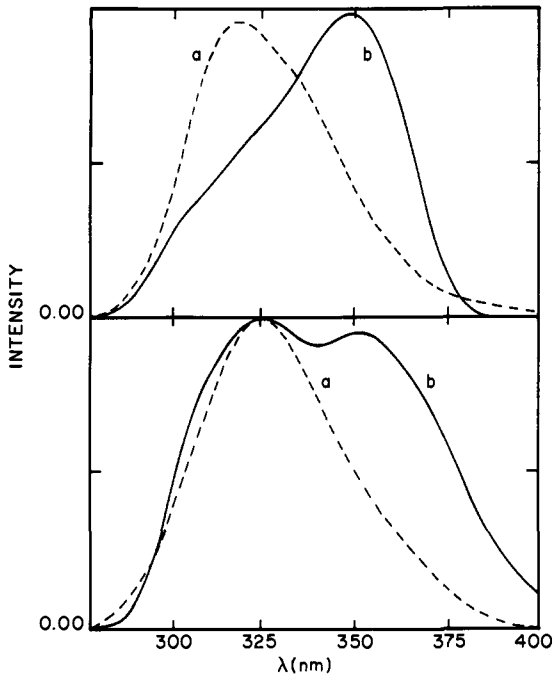

Figure 5. Excitation profiles for $Cu_4I_4(py)_4$ in toluene solution at 294 K (lower) and at 77 K (upper). Curves labeled "a" are the excitation spectra monitoring at the LE λ_{max} (excitation maxima at 325 (294 K) and 317 nm (77 K)) and "b" are the excitation spectra monitoring at the HE λ_{max} (excitation maxima at 325 and 352 nm (294 K) and at 350 nm (77 K)).

reflecting an environment less rigid than the solid state (λ_{max} = 580 nm) or 77 K toluene glass (583 nm) but more rigid than 294 K toluene solution (690 nm).

The excitation profiles of the two emission bands of I in 294 K toluene solution are shown in Figure 5. That for the LE band exhibits λ^{ex}_{max} at 325 nm. The excitation profile of the HE band exhibits λ^{ex}_{max} at both 325 and 352 nm. A similar λ^{ex} dependence was observed in a 77 K toluene glass. The LE emission monitored at 583 nm achieves maximum intensity at λ^{ex}_{max} 317 nm, while the HE emission monitored at 436 nm exhibits a λ^{ex}_{max} at 350 nm with a shoulder at ~310 nm.

In 294 K benzene, the emission spectrum of the dinuclear species $Cu_2I_2(Et_4en)_2$ displayed a single broad band centered at 640 nm (E^{00} = 19.7 kK).

C. **Time-Resolved Emission Spectra.** Time-resolved spectroscopy has been used to demonstrate the disparate temporal behavior of the HE and LE emission bands of the $Cu_4I_4(py\text{-}x)_4$. The time-resolved spectra of $Cu_4I_4(py)_4$ in 294 K toluene solution are depicted in Figure 6. Similar behavior was seen for all the substituted pyridine complexes.[1,3a] In each case, the HE band intensity was found to be comparable to that of the LE band at short delay times (τ < 60 ns) after 337-nm laser excitation. The HE emission decays much more rapidly (see below) so was not detectable at μs delay times.

Time-resolved spectroscopy was also used to probe the temporal luminescence behavior of I in THF solution. Two poorly resolved LE bands were observed at ~685 and ~720 nm (uncorrected). However, the intensity at 720 nm decayed more rapidly than that at 685 nm, suggesting the presence of at least two species, perhaps the result of some pyridine displacement by this donor solvent.

D. Emission Lifetimes. Solid-State Materials. The emission lifetimes of various $Cu_4I_4L_4$ as solid powders at 294 and 77 K are presented in Table V. The HE emission, not detectable at room temperature, was observed as an exponential decay at 77 K, but only for L = py-x. When monitored at the LE λ_{max}, luminescence decays were exponential at room temperature and at 77 K. A brief examination of the temperature dependence of I using time-resolved spectroscopy (λ^{ex} = 355 nm) showed only the LE band at $T \geq 150$ K (λ_{max} 570 nm, uncorrected, τ = 12.1 μs) but both the HE and LE bands to be measurable at 100 K (λ_{max} = 433 and 600 nm, τ = 0.50 and 16.6 μs, respectively). From Table V, it is clear that for the $Cu_4I_4L_4$ solids, the LE emission τ's are relatively temperature insensitive and increase only about 2-fold between room temperature and 77 K.

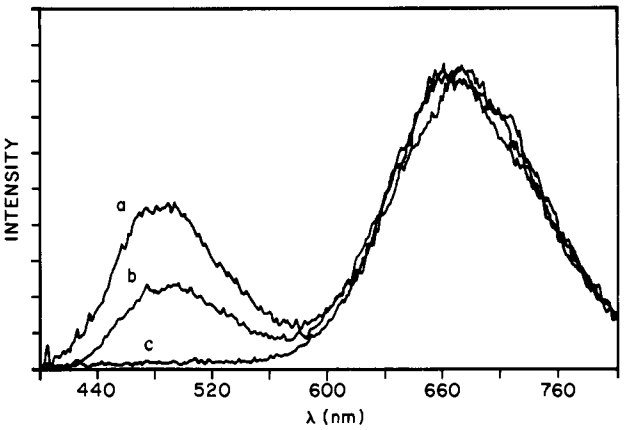

Figure 6. Time-resolved spectra of $Cu_4I_4(py)_4$ in 294 K toluene solution with 337-nm excitation. Delay times are (a) 42.5 ns; (b) 200 ns; and (c) 1.14 μs.

Table V. Emission Lifetimes of Various $Cu_4I_4L_4$[a]

L	solvent	T (K)	$\tau_{(HE)}$,[b] in μs	$\tau_{(LE)}$,[c] in μs
pyridine	solid	294	*d*	11.1
		77	23.2	25.5
	toluene	294	0.45	10.6
		250	0.91	16.9
		231	1.76	21.2
		195	5.21	26.1
		77	32.9	26.5
	methyl acetate	294	*d*	4.4
	CH_2Cl_2	294	0.076	3.16
	DMTHF	294	*d*	7.98
	THF	294	*d*	1.5 (6.8)[e]
py-d_5	solid	294	*d*	11.1
		77	20.8	24.0
	toluene	294	0.22	14.1
		250	0.65	21.3
		231	1.28	25.1
		195	3.19	31.1
		77	42.3	44.2
4-Phpy	toluene	294	0.12	9.4
		250	0.30	17.4
		195	5.46	24.2
		77	63.0	38.4
4-*t*-Bupy	solid	294	*d*	18.8
		77	29.2	38.8
	toluene	294	0.35	10.3
		273	0.54	12.4
		231	1.41	20.2
		195	4.75	24.8
		77	38.7	43.5
4-$PhCH_2$py	toluene	294	0.56	11.0
3-Cl-py	toluene	294	0.35	12.7
piperidine	solid	294	*d*	12.3
		77	*d*	13.4
	toluene	294	*d*	0.11
		250	*d*	0.138
		231	*d*	0.165
		195	*d*	0.199
		77	*d*	19.8
morpholine	toluene	294	*d*	0.51
P(*n*-Bu)$_3$	toluene	294	*d*	2.23

[a] Lifetimes in μs. Experimental uncertainties are ≤±10%. [b] Lifetime measured at the λ_{max} of the HE emission band. [c] Lifetime measured at the λ_{max} of the LE emission band. [d] HE band not observable. [e] Two LE emissions observed, see text.

Solution Lifetimes. Independent measurements of the excited-state emission lifetimes made with two different instruments gave identical results and were consistent with the observed time-resolved spectral measurements described above. The

emission lifetime data for various $Cu_4I_4L_4$ in solution are summarized in Table V and represent exponential decays when monitored at emission maxima with the exception of the LE emission for I in THF which was best fit to a biexponential.

With regard to the LE emissions, the following general observations may be made. At room temperature, the τ values measured for the various Cu_4I_4(py-x)$_4$ derivatives in toluene solution proved to be relatively insensitive to the nature of the pyridine substituent, all falling into the range 9–14 μs. Indeed these values did not differ very significantly from the $\tau_{(LE)}$ values measured for the solids at 294 K. Lowering T did lead to longer LE emission lifetimes; however, the roughly 3–4-fold increase in τ at 77 K is relatively modest given >200° difference in temperature. The $\tau_{(LE)}$ values measured in 294 K toluene solution for the complexes of the saturated amines piperidine and morpholine were factors of 100 and 20 shorter than for the Cu_4I_4-(py-x)$_4$ analogues, although, in the solid state, the lifetime for II was comparable to that of I. For II, lowering T to 195 K had a modest effect; however, further decreasing T to 77 K (below the glass transition) increased $\tau_{(LE)}$ by two orders of magnitude.

The HE emission was observed only for the aromatic amine clusters Cu_4I_4(py-x)$_4$, and the measured lifetimes in ambient temperature solution of this weak emission proved to be nearly two orders of magnitude shorter than the respective $\tau_{(LE)}$ values. Furthermore, the variations in the $\tau_{(HE)}$ values for various pyridine substituents x is substantial, varying over the range 120–560 ns for the limited number of species investigated. Lowering the temperature to 77 K leads to increases in $\tau_{(HE)}$ by more than two orders of magnitude.

Emission Risetimes. Close inspection of the temporal emission behavior of Cu_4I_4(4-Phpy)$_4$ in 294 K toluene revealed an unexpected rise in the LE emission intensity in the very early stages of the luminescence profile. The *risetime* was measured to be about 20 ± 1 ns, close to the response time of the YAG laser (λ_{1n}^{ex} 355 nm) and electronics used to carry out these investigations. For this reason the LE emission signal risetimes under these conditions were compared to those of two other well-characterized emitters. The first was DCM laser dye (τ = 1.31 ns),[38] the emissioin from which should follow the laser profile closely; the second was $[Ru(bpy)_3]Cl_2$ in aqueous solution. These comparisons demonstrated that the emission intensity of Cu_4I_4(4-Phpy)$_4$ continues to rise after the laser pulse is complete and after the "prompt" emitter $[Ru(bpy)_3]Cl_2$ attained maximum intensity.[39] The risetime did not exhibit an emission wavelength dependence (650–850 nm), remained constant as laser pulse power was varied, and was not dependent on which PMT was used (RCA 8852 vs EMI 9816A). No such risetime was observed for the HE emission from the same solutions. Thus, instrumental artifacts were excluded as being responsible for this unusual behavior.

The risetime of the LE emission was not dependent on $[Cu_4I_4$(4-Phpy)$_4]$ in toluene over the range 1.2×10^{-3}–3.0×10^{-5} M but was temperature-dependent (Figure 7 with τ_{rise} values of 20 ns (293), 38 ns (273), 195 ns (250), 910 ns (231), and 2.59 μs (195 K). Furthermore, such behavior was not exclusive to the 4-Phpy complex but was also seen for I (τ_{rise} values of 22 ns, 94 ns, and 1.02 μs at 231, 195, and 77 K, respectively) and for Cu_4I_4(tbpy)$_4$ (75 and 600 ns at 195 and 77 K, respectively) in toluene solution but only at lower T. Solid samples of all these complexes exhibited prompt LE emissions at 77 K, and solutions of II in toluene also exhibited prompt LE emission over the temperature range 77–294 K.

E. Emission Quantum Yields. The emission quantum yields Φ_e of various Cu_4I_4(py-x)$_4$ clusters in 294 K toluene solution were determined as described in the Experimental Section under conditions identical with those described for the lifetime and spectral measurements. The measured values are reported in Table VI. (The Φ_e value reported here for I is about twice that previously reported.[12]) The range in the Φ_e(LE) values is relatively small, 0.034–0.17 for the substituted pyridine complexes, but Φ_e for the shorter lived LE emission of Cu_4I_4(piperidine)$_4$ is much smaller. The Φ_e(LE) value for I proved to be modestly solvent-dependent, giving values of 0.053, 0.043, and 0.021 in DMTHF, CH_2Cl_2, and THF, respectively. The Φ_e's also proved sensitive to O_2. Saturation of a 294 K toluene solution of I with O_2 (9×10^{-3} M)[40] led to a drop in the Φ_e(LE) value to 0.0013. Purging with purified N_2 restored this to 0.09.

Table VI. Emission Quantum Yields for $Cu_4I_4L_4$ in 294 K Toluene

L	$\Phi_{e(LE)}$	$\Phi_{e(LE)}/\tau_{(LE)}$[a]	$\Phi_{e(HE)}$
pyridine	0.090	8.3×10^3	3.4×10^{-4}
py-d_5	0.11	8.3×10^3	3.7×10^{-4}
4-Phpy	0.060	6.4×10^3	5.8×10^{-3}
4-*t*-Bupy	0.17	1.65×10^4	1.8×10^{-3}
4-$PhCH_2$py	0.073	6.6×10^3	*b*
3-Cl-py	0.034	2.7×10^3	*b*
piperidine	2.4×10^{-4}	2.2×10^3	*c*

[a] LE quantum yields measured by using $Ru(bpy)_3Cl_2$ as a reference. HE quantum yields measured by using the corresponding $\Phi_{e(LE)}$ as an internal reference. λ^{ex} = 350 nm. Error is ±5%. [b] $\Phi_{e(HE)}$ not measured. [c] HE emission not observed.

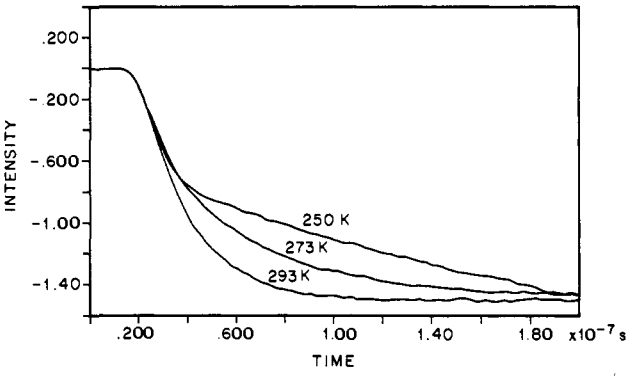

Figure 7. Temperature dependence of risetimes for LE emission from Cu_4I_4(4-Phpy)$_4$ in toluene at 690 nm: τ_{rise} = 20 ns (293 K), 38 ns (273 K), 195 ns (250 K).

Quantum yields for the HE emissions in 294 K toluene for various Cu_4I_4(py-x)$_4$ complexes proved to be about two orders of magnitude smaller than the respective Φ_e values for LE emission. These values are also summarized in Table VI.

F. Emission Lifetime Quenching. Quenching by Lewis Bases. Addition of pyridine to a solution of I in dry, deaerated benzene led to systematic decreases in the HE emission lifetime, while the LE lifetime remained invariant within experimental uncertainty. Figure 8 depicts the Stern–Volmer plot[32] of τ_0/τ vs [py], where τ_0 is the HE lifetime in the absence of pyridine (452 ns) at 294 K. The plot is linear with an intercept of 1.01 ± 0.06 and a slope (K_{SV}) of 270 ± 10 M^{-1}. Given that $K_{SV} = k_q\tau_0$, the bimolecular quenching constant k_q was calculated to be $5.9 \pm 0.5 \times 10^9$ M^{-1} s^{-1}.

The Stern–Volmer quenching of the HE emission from I was examined at several different temperatures. Notably, k_q decreases with increasing T {$k_q = 5.9 \pm 0.5 \times 10^9$ (294 K), $3.5 \pm 0.7 \times 10^9$ (303 K), and $2.9 \pm 0.5 \times 10^9$ (308 K) M^{-1} s^{-1}} in a manner similar to that reported by McMillin for the quenchiing of the MLCT emission lifetime of $Cu(dmp)_2^+$ (dmp = 2,9-dimethyl-1,10-phenanthroline) by Lewis bases.[41] The respective ΔH^* and ΔS^* calculated from these data are −9 ± 2 kcal mol^{-1} and −50 cal mol^{-1} K^{-1}.

The effect of pyridine substituents in the sterically significant ortho position was demonstrated by using 2,6-dimethylpyridine (lutidine) and 2,6-di-*tert*-butylpyridine (dtbpy). Stern–Volmer plots for these two bases (Figure 8) gave the respective k_q values

(38) Speiser, S.; Shakkour, N. *Appl. Phys. B* **1985**, *38*, 191–197.
(39) The luminescent MLCT state of $Ru(bpy)_3Cl_2$ is populated from upper levels within 0.1 ns (Brettel, K.; Schlodder, E. *Rev. Sci. Instrum.* **1988**, *59*, 670–671).
(40) Evans, F. D.; Battino, R. *J. Chem. Thermodyn.* **1971**, *3*, 753–760.
(41) (a) Palmer, C. E. A.; McMillin, D. R.; Kirmaier, C.; Holten, D. *Inorg. Chem.* **1987**, *26*, 3167–3170. (b) Stacy, E. M.; McMillen, D. R. *Inorg. Chem.* **1990**, *29*, 393–396.

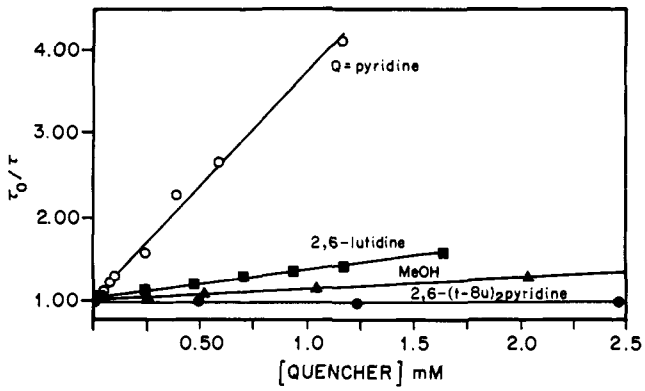

Figure 8. Stern–Volmer plots for the quenching of the HE emission from $Cu_4I_4(py)_4$ by different Lewis bases in benzene at 294 K.

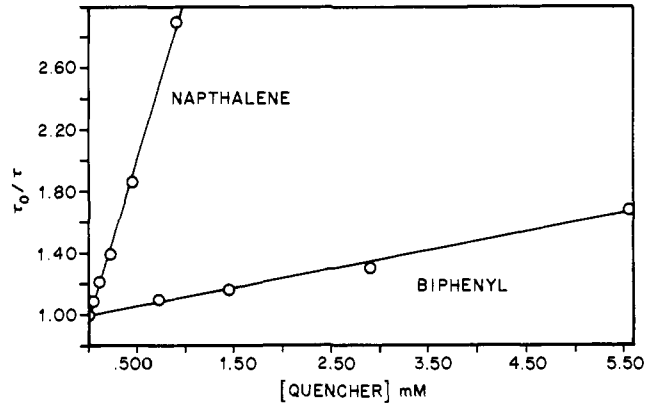

Figure 9. Stern–Volmer plots for the quenching of the HE emission from $Cu_4I_4(py)_4$ by different aromatic energy acceptors at 294 K.

$9.5 \pm 0.9 \times 10^8$ and $<10^6$ M^{-1} s^{-1}, results consistent with the inhibition of the quenching mechanism by bulky ortho substituents. An attempt to use 2,6-diphenylpyridine as a sterically hindered Lewis base was precluded due to the existence of a bright blue emission from the quencher itself which resulted in phototube (RCA 8852) saturation. Although, k_q may be estimated at 2×10^9 M^{-1} s^{-1} from two low concentration data points, it is likely that this quenching operates by a different mechanism (see below). In addition, quenching of the HE emission is not limited to aromatic amines. Methanol also proved to be a quencher and gave a linear τ_0/τ vs [MeOH] Stern–Volmer plot (Figure 8) from which $k_q = 4.4 \pm 0.5 \times 10^8$ M^{-1} s^{-1} in benzene solution was calculated.

Quenching by Energy Acceptors. The HE emission lifetime also proved to be sensitive to added energy acceptors. Addition of biphenyl (E_T = 23.0 kK),[42] naphthalene (E_T = 21.3 kK),[42] or O_2 (E_T = 7.8 kK)[42] to deaerated 294 K benzene solutions of I resulted in dynamic quenching of the HE emission. For the first two, there was no effect on the LE emission lifetimes, but dynamic quenching of the LE emission was seen for solution containing O_2. Linear Stern–Volmer plots for biphenyl and naphthalene (Figure 9) were used to determine the respective k_q's $3.5 \pm 0.2 \times 10^8$ and $6.6 \pm 0.1 \times 10^9$ M^{-1} s^{-1} for quenching of the HE state. For O_2, k_q values of $\geq 10^{10}$ M^{-1} s^{-1} for HE emission quenching and $k_q = 6.0 \pm 0.6 \times 10^8$ M^{-1} s^{-1} for LE emission quenching were estimated from a single [O_2] experiment. The observation of dynamic quenching of the LE emission only by oxygen is consistent with this being the one acceptor in the series with an E_T lower than the estimated energy of the LE state (17.5 kK, Table III).

Concentration Quenching. During the quenching studies, the HE emission lifetime proved to be sensitive to the concentration of $Cu_4I_4(py)_4$, yet the LE emission lifetime was invariant over the same range of conditions. Figure 10 demonstrates the linear

(42) Murov, S. L. *Handbook of Photochemistry*; Marcel Dekker: New York, NY, 1973; pp 27–35.

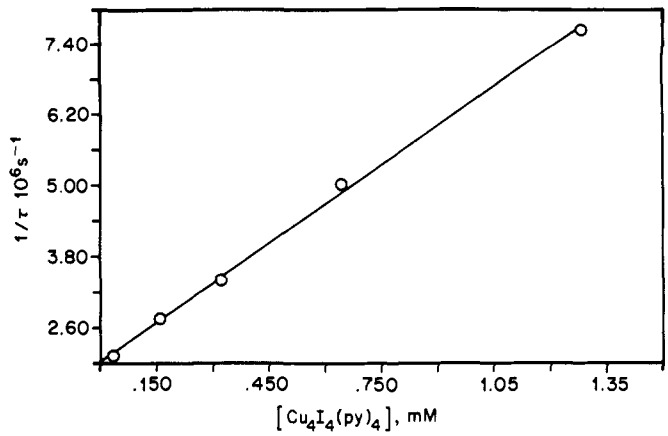

Figure 10. Stern–Volmer plots for the self-quenching of the HE emission from $Cu_4I_4(py)_4$ at 294 K.

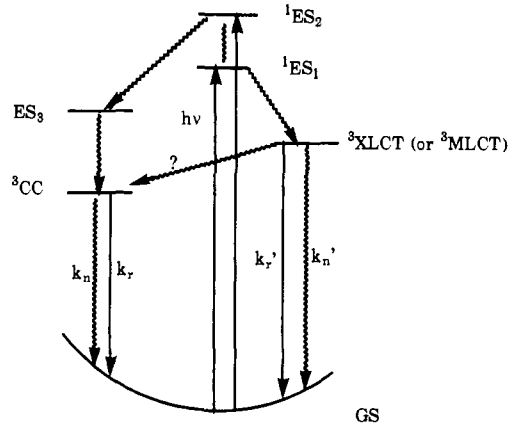

Figure 11. Qualitative excited-state diagram for $Cu_4I_4(py\text{-}x)_4$.

dependence between [I] and the reciprocal of the lifetime (τ^{-1}). The slope of this plot gives the self-quenching constant $k_q^s = 4.5 \pm 0.5 \times 10^9$ M^{-1} s^{-1} and an intercept (τ_0^{-1}) of $2.2 \pm 0.2 \times 10^6$ s^{-1} from which was calculated $\tau_0 = 0.45 \pm 0.04$ μs. Linear Beer's law plots (e.g., Figure 1) were obtained over this same concentration range at all wavelengths monitored between 300 and 370 nm. In addition, a similar plot of self quenching in the presence of pyridine ([py] = 2.2×10^{-4} M) in benzene gave a k_q^s value (4.4×10^9 M^{-1} s^{-1}) identical with that above determined in the absence of added pyridine.

Discussion

A. Assignment of Emission Bands. The Higher Energy (HE) Bands. Three general observations point to the charge-transfer nature of these bands. First, the HE bands are observed only for $Cu_4I_4(py\text{-}x)_4$ clusters and are not present in the emission spectra of the structurally analogous saturated amine clusters $Cu_4I_4A_4$ where A = morpholine and piperidine (Tables II and III). Thus empty π-symmetry orbitals such as the pyridine π-antibonding MOs are a necessary requirement for observing these bands. Second, the HE band energies are quite sensitive to substituents on the pyridines; electron-withdrawing substituents shift these to lower values (Table III). Third, the HE band for I in solution is sensitive to the nature of the solvent; donor solvents shift this band to higher energy. Such observations led to our original conclusion[3a] that the emission band could be attributed to a metal-to-ligand charge-transfer (MLCT) excited state in agreement with previous discussions by Holt[11] and others of the low-temperature emission spectra of crystalline I.

Nonetheless, while the above characteristics clearly point to the acceptor orbital(s) in the excited state responsible for the HE emission being the empty π-symmetry orbitals of py-x, it is not clear what is the nature of the donor orbital. Preliminary ab initio calculations in this laboratory have concluded that for the hypothetical cluster $Cu_4I_4(NH_3)_4$ the highest occupied MOs are not

metal-centered but are >80% iodide p-orbitals in character.[43] The metal d-orbital contribution to the HOMO is small, and those MOs which have substantial metal character are much lower in energy. Further calculations of smaller fragments such as CuIpy and $Cu_2I_2py_2$ (in geometries consistent with those occupied by the atoms in the clusters) support this conclusion, although there is a greater metal contribution to the HOMO in this case.[44] We are thus led to conclude that an MLCT assignment may be a bit naive and that a more realistic assignment would be that this excited state is largely iodide → py-x, i.e., *a ligand-to-ligand charge transfer* (XLCT, where X represents the halogen) in character. However, as a caveat, the quenching behavior of the HE emission in the presence of Lewis bases[3b] (see below) is suggestive of an ES for which the metal center is more electrophilic than in the GS, as would be expected for a MLCT state.

XLCT excited states have received attention in photophysical studies[4a,45] of Zn(II) complexes of the type ZnX_2(phen) (where phen is 1,10-phenanthroline and X is a halide or organic sulfide RS^-), and L'LCT states have been invoked[46] as being responsible for the unusual photophysical properties of some Re(I) complexes of the type $Re(CO)_3$(bpy)(py-PTZ)$^+$ (where bpy is 2,2'-bipyridine and PTZ is phenothiazine). Other examples of XLCT excited states are documented in a recent review[47] which also draws the analogy between such excited states in metal complexes and the well-known charge-transfer transitions seen in pyridinium halide ion pairs, e.g., $[RNC_5H_5^+]\cdots X^-$.[48] Obviously, the Cu_4I_4(py-x)$_4$ clusters fit this analogy quite well.

Lower Energy (LE) Emission Bands. The LE bands of the $Cu_4I_4L_4$ clusters can be assigned to the emission from excited states characteristic of the Cu_4I_4 core, since observation of this band is independent of whether L is a saturated amine or a pyridine,[12] and the LE band energies for various Cu_4I_4(py-x)$_4$ are independent of the substituent x[3a] (Tables II and III). On this basis, an assignment of the emitting state as a MLCT or XLCT ES would be unlikely, and both Holt[11] and Vogler[12] have assigned the LE band of $Cu_4I_4L_4$ as originating from a metal-centered $3d^94s^1$ ES modified by the copper–copper interactions in the Cu_4I_4 core, which we earlier chose[3] to designate as a metal-cluster centered (MCC) ES. A similar assignment has been offered for the emitting states of clusters of several other d^{10} metals.[49] For such an excited state, the very large Stokes shift from the excitation maxima (Figures 2 and 5) to the LE emission λ_{max} (9.1 kK for solid I at 294 K, 16.3 kK for toluene solution; in contrast the Stokes shift for the HE band in room temperature toluene was 4.6 kK) can be rationalized by a strong distortion in going from the ground state, which has at most weak metal–metal bonding between the d^{10} Cu(I) centers[50] to the ES where metal–metal bonding should be enhanced by depopulation of a σ_{MM}^* d-orbital concurrent with population of a σ_{MM}^b "s" type orbital. While this assignment appears to be consistent with the insensitivity of the LE band energy to the nature of L and to solvent polarity, it does run counter to the conclusions of the ab initio calculations,[43,44] which suggest the HOMO to be principally iodine 5p in character and the LUMO to be principally copper 4s in character. This would suggest a I → Cu (or more correctly a I_4 → Cu_4) halide-to-metal charge-transfer (XMCT) excited-state assignment. Since the LUMO would remain σ-bonding with regard to the Cu_4 core, this ES would also be expected to display substantial distortion from the GS configuration, hence it would be expected to display large Stokes shifts in the emission bands. Such a transition would still be considered to be cluster-centered (CC), although the designation "metal cluster centered" may no longer seem appropriate. (Previous workers have assigned emission from low-temperature (4.2 K) CuI crystals to donor–acceptor pairs,[51] although the wavelength of the emission (420 nm) in that case is much shorter than that from the $Cu_4I_4L_4$ clusters described here.)

In the context of the above assignment, it is notable that $Cu_4Cl_4py_4$, the chloride analogue of I, displays only a single emission band,[52] and this occurs at higher energy (λ_{max} 519 nm in the 77 K solid). The energy of this band would be qualitatively consistent with the MLCT assignment; furthermore, no emission was seen from Cu_4Cl_4(morpholine)$_4$, and the emission observed for Cu_4Cl_4(Phpy)$_4$ is considerably shifted to the red (λ_{max} = 610 nm),[52] both behaviors being in contrast with those of the LE band of the $Cu_4I_4L_4$ clusters. These observations suggest that assignments of the single emission bands seen for the Cu_4Cl_4(py-x)$_4$ clusters are likely to be different from those of the LE bands of the respective iodide analogues. The details of the chloride complexes will be discussed elsewhere.[52]

B. Dynamics of Emitting States. Another distinctive feature of the LE emissions observed for each of the Cu_4I_4(py-x)$_4$ clusters is the relatively long lifetime τ, which proved to be independent of the nature of the ligand substituent x and relatively independent of the medium and of the temperature (Table V). The latter seems particularly striking given the marked shifts in λ_{max} as the temperature, and the rigidity of the media were changed (Table III). The LE emission quantum yield for each of these clusters was relatively large, (0.03 → 0.17) for the py-x species with only the saturated amine complex II giving a much smaller value (Table VI). Given the absence of information regarding the efficiency of the internal conversion/intersystem crossing processes populating the emitting LE state, it is pointless to make quantitative comparisons of the relatively minor differences in $\Phi_{e(LE)}$ except to note that the ratio $\Phi_{e(LE)}/\tau_{(LE)}$ for II is within the same order of magnitude as those ratios taken for the py-x clusters. Since this ratio should be more reflective of the relative radiative rate constants, this comparison suggests that the short lifetime and small quantum yield for toluene solutions of $Cu_4I_4L_4$, when L = the saturated amine piperidine, can be attributed to a higher rate of nonradiative deactivation from II. One cause of a higher k_n may be the presence of a N–H bond at the coordinating piperidine nitrogen, given that the proximity of high-frequency vibrational oscillators often enhance nonradiative deactivation from metal-centered excited states.[53]

A particularly distinctive feature of the photophysical behavior of Cu_4I_4(py-x)$_4$ clusters is that, under all conditions investigated, the HE and LE excited-state emissions appeared to operate independently with substantially different lifetimes and excitation spectra. Such observations are rare for a single pure compound and tempt one to attribute the two emissions to the presence of two different chemical species, especially in the context of the lability of the Cu(I) species demonstrated by the NMR experiments. However, the parallel behavior of well-characterized crystalline solids, the linear Beer's law plots of $Cu_4I_4L_4$ solutions, etc., argue strongly for the photophysical behavior in solution also being characteristic of well-defined tetranuclear clusters. Similar behavior has been described by other workers for related tetranuclear clusters of Cu(I).[13]

The poor coupling between the HE and the LE excited states may be best explained by large distortions along different coordinates for the respective states. XMCT excitation to give the LE ES should lead to contraction of the Cu_4 core and perhaps to some expansion of the I_4 core, while XLCT excitation to give

(43) Kyle, K. R.; Palke, W. E.; Ford, P. C. *Coord. Chem. Rev.* **1990**, *97*, 35–46.
(44) Vitale, M.; Palke, W. E.; Ford, P. C. Studies in progress.
(45) Truesdell, K. A.; Crosby, G. A. *J. Am. Chem. Soc.* **1985**, *107*, 1787–1788.
(46) Chen, P.; Westmoreland, T. D.; Danielson, E. R.; Schanze, K. S.; Anthon, D.; Neveux, P. E.; Meyer, T. J. *Inorg. Chem.* **1987**, *26*, 1116–1126.
(47) Vogler, A.; Kunkeley, H. *Comments Inorg. Chem.* **1990**, *9*, 201–220.
(48) Kosower, E. M. *Prog. Phys. Org. Chem.* **1965**, *3*, 81–163.
(49) Vogler, A.; Klunkely, H. *Chem. Phys. Lett.* **1988**, *150*, 135–137; **1989**, *158*, 74–76; **1989**, *164*, 621–624.
(50) (a) Mehrota, P. K.; Hoffmann, R. *Inorg. Chem.* **1978**, *17*, 2187. (b) Trogler, W. C.; Lee, S. W. *Inorg. Chem.* **1990**, *29*, 1659–1662.
(51) Vereshchagin, I. K.; Nikitenko, V. A.; Stoyukhin, S. G. *J. Lumin.* **1984**, *29*, 215–221.
(52) Ryu, C. K.; Kyle, K. R.; Ford, P. C. Manuscript in preparation.
(53) (a) Ryu, C. K.; Lessard, R. B.; Lynch, D.; Endicott, J. F. *J. Phys. Chem.* **1989**, *93*, 1752–1758. (b) Kober, E. M.; Caspar, J. V.; Lumpkin, R. S.; Meyer, T. J. *J. Phys. Chem.* **1986**, *90*, 3722–3734.
(54) (a) Emission studies (ref 54b) have established E^{00} values for the ligand-centered $^3\pi\pi^*$ ES of pyridinium (pyH^+), 2,6-dimethylpyridine, and 2,6-dimethylpyridinium ion to be 29.7, 28.3, and 28.6 kK, respectively. (b) Motten, A. G.; Kwiram, A. L. *J. Chem. Phys.* **1981**, *75*, 2608–2615.

the HE ES would lead to some shortening of Cu–L bonds accompanied by lengthening of Cu–I distances. Preliminary results of ab initio calculations of changes in the cluster bonding upon ES formation are consistent with these qualitative suggestions.[44] The poor coupling between these states is further reflected by the observation of a *risetime* in the LE emission, a feature which is particularly evident for the $Cu_4I_4(4\text{-Phpy})_4$ cluster but also observed with several others. Since the HE emission did not display a similar risetime and since this risetime is considerably shorter than $\tau_{e(HE)}$ under the same conditions, it appears that a third, spectroscopically unobservable, higher energy state is the direct predecessor to the LE ES. One possibility would be a triplet ligand-centered $\pi\pi^*$ state.

These conclusions are illustrated by the qualitative excited-state diagram shown in Figure 11. The relatively long lifetimes of both the higher and lower energy emissions are suggestive of triplet spin-state assignments for the emitting excited states. With regard to the excitation spectra, a key feature is that the peaks observed fall on the near-UV tail of the absorption spectra of these compounds (Figures 1 and 5). Excitation at longer λ^{ex} ($\sim$360 nm) appears to populate preferentially the state (ES_1) which is the principal predecessor to the HE emission, while excitation at a somewhat shorter wavelength ($\sim$330 nm) populates (principally) ES_2, presumably a cluster-centered state of XMCT character, a predecessor of the LE emission. However, the observed risetime suggests that a third state ES_3 is the direct predecessor of the emitting ^{3}CC state, since it is improbable that ES_1 prepared by direct excitation would be sufficiently long-lived to explain the risetime. Furthermore, since $\tau_{risetime}$ is much shorter than $\tau_{(HE)}$, ^{3}XLCT (MLCT) cannot be ES_3. Ligand-centered triplet $\pi\pi^*$ ES of the pyridine(s) are logical candidates for ES_3 since their energies fall into the appropriate range.[54] Indeed, poor coupling between ligand-centered $^3\pi\pi^*$ and MLCT ES of the Cu(I) complex Cu(phenanthroline)$(PPh_3)_2^+$ have been reported.[7e] Given the magnitude of the Stokes shifts observed in these cases, we believe it is likely that the energy differences between ES_2, ES_3, and ^{3}CC and the origin of the slow interconversion between ES_3 and ^{3}CC lie in structural distortions once these species undergo excitation. The poor communication between the ^{3}XLCT and ^{3}CC states is another reflection of the probable differences in the structures of these two types of states.

C. **Bimolecular Quenching of Cluster Excited States.** Addition of pyridine to solutions of I in benzene leads to dynamic quenching ($k_q = 5.9 \times 10^9$ M^{-1} s^{-1}) of the HE emission with no significant effect on the LE emission band. Quenching by the sterically demanding Lewis base 2,6-dimethylpyridine (lutidine) is a factor of six slower, while no quenching was detectable for the much more sterically demanding 2,6-di(*tert*-butyl)pyridine (Figure 8). Methanol also serves as a HE quencher with k_q about an order of magnitude smaller than for py. None of these quenchers have a low-energy ES which would allow energy-transfer quenching (e.g., $E_T = 29.7$ kK for py).[54] In earlier studies, McMillin et al. have noted the Lewis base quenching of the MLCT emission from $Cu(dmp)_2^+$ in CH_2Cl_2 solution (dmp = 2,9-dimethyl-1,10-phenanthroline) and attributed this to coordination by the Lewis base to the, formally Cu(II), metal center of the MLCT state leading to marked increases in nonradiative deactivation rates.[7a-c] The behavior of the $Cu(dmp)_2^+$ system is consistent with the HE quenching described here for I, namely, substantial kinetic effects were noted for pyridines substituted in sterically sensitive ortho positions, and pyridine proved to be more than an order of magnitude more effective as a quencher than is methanol. Furthermore, the $\Delta H_q^{\ddagger}$ values determined for both systems are negative. Thus, in analogy to the mechanism proposed for quenching of $Cu(dmp)_2^+$, the formation of an ES complex as in eq 2 would appear to be a logical explanation of these observations

$$\begin{array}{ccc} I^{**} + B & \overset{K_e}{\rightleftharpoons} & (IB)^{**} \\ \downarrow k_d^0 & & \downarrow k_{ib} \\ I & & I + B \end{array} \qquad (2)$$

(where I** is the HE excited state of I, B the Lewis base, and (IB)** the excited-state complex). According to this model, the deactivation rate constant defined by

$$k_d = (\tau)^{-1} \qquad (3)$$

would be determined by the sum of the unimolecular and bimolecular processes

$$k_d = k_d^0 + k_{ib}K_e[B] \qquad (4)$$

where the product $k_{ib}K_e$ would equal the k_q measured for the various Lewis base quenchers. In this case, $\Delta H_q^{\ddagger} = \Delta H_e + \Delta H_{ib}^{\ddagger}$; a negative ΔH_e for the equilibrium could give an overall negative value for $\Delta H_q^{\ddagger}$.

The basic ambiguity of the above interpretation is that the $Cu(dmp)_2^+$ system for which the exciplex quenching mechanism was first proposed emits from an ES which has been assigned as MLCT in character; therefore, a process involving attack by a Lewis base on a metal center which is more electrophilic in the ES would appear quite reasonable. However, it is not clear what site should show analogously enhanced electrophilicity toward Lewis bases if the HE state of I is XLCT in character. Several possibilities exist. One might be that the ab initio calculations simply underestimate the contributions of the metal d-orbitals to the HOMO. An alternative is that, in the course of relaxing from the initially formed Franck–Condon state, the resulting emitting state has more MLCT character than shown by calculations based on the GS nuclear configurations.

Selective quenching of the HE emission (leaving the LE emission unaffected) of I was also accomplished with the aromatic hydrocarbon energy acceptors biphenyl and naphthalene which have the respective triplet energies 23.0 and 21.3 kK,[42] i.e., between the estimated E^{00} values for the HE (24.5 kK) and the LE (17.5 kK) excited states (Table III). In contrast, the $^1\Delta$ state of O_2 has a much lower energy (7.8 kK), and quenching of the HE and LE emissions occurs with the respective k_q's $>10^{10}$ and 6×10^8 M^{-1} s^{-1}.

The self-quenching of the HE emission demonstrated by Figure 10 again is unusual especially in the context that only the HE emission is affected. One potential explanation of this phenomenon might be that varying [I] might lead to increased concentrations of free py owing to the possible equilibrium

$$Cu_4I_4(py)_4 \leftrightarrow Cu_4I_4py_3^{\cdot} + py \qquad (5)$$

In such a case, quenching might occur by the Lewis base mechanism. However, the py dissociation equilibrium constant required for this model would be too large to be consistent with the linear Beers law plots as in Figure 1. Furthermore, the self-quenching constant proved to be independent of significant concentrations of free pyridine added to the solution. Thus, we propose that the self quenching of the HE emission is the result of bimolecular energy transfer from one cluster to another to quench the HE ES of the first and to form the LE ES of the latter. While one might predict enhanced LE emission under such circumstances, none was observed; however, this was no surprise given the much lower yield of emission from the HE states. That the HE state can be quenched thus by bimolecular energy transfer at rates competitive to unimolecular internal conversion to the lower energy states is further illustration of the poor coupling between these two different types of ES in these clusters.

In Summary. The spectral and lifetime data reported here for a number of different $Cu_4I_4L_4$ clusters, media, and conditions all point to a complex series of different excited states which are poorly coupled. These properties presumably find their origin in structural differences between different states owing to the population of $\sigma_{MM}{}^b$ orbitals in formation of the cluster-centered ^{3}CC states. Although the assignments of relevant excited states are certainly not unequivocal, it appears that the potential importance of the halide orbitals in determining the character of these states may have been underestimated, although not ignored, in earlier an discussion of the remarkably rich photophysical properties of these readily accessible compounds.

Acknowledgment. This research was supported by the U.S. National Science Foundation (Grant No. CHE 87-22561). Dr. John A. DiBenedetto, now at EG&G, Santa Barbara, made major contributions in the early stages of the research described in this manuscript. K.R.K. was the recipient of a University of California Special Regents Graduate Fellowship. We thank Professor R. J. Watts of this department for allowing the use of instrumentation for time-resolved spectral measurements and Christine Miller of this department for help in making such measurements. The contributions of Jerald A. Simon of this research group in modifying the computational hardware and software for excited-state lifetime measurements were incalculable.

Synthesis and Characterization of Macrobicyclic Iron(III) Sequestering Agents[1]

Thomas M. Garrett, Thomas J. McMurry, Mir Wais Hosseini, Zelideth E. Reyes, F. Ekkehardt Hahn, and Kenneth N. Raymond*

Contribution from the Department of Chemistry, University of California, Berkeley, California 94720. *Received February 12, 1990. Revised Manuscript Received October 16, 1990*

Abstract: This paper reports the template and high-dilution syntheses of a series of macrobicyclic iron(III) sequestering agents based on catechol as the ligating group. An X-ray structure of the salt denoted as Na_3[Fe(bicappedTRENCAM)]·17.5H_2O is the first for any ferric tricatechoyl amide and displays an unprecedented trigonal prismatic coordination (C_{3h} symmetry) for the ferric ion. The compound crystallizes in space group $P6_3/m$ with a = 13.785 (3) Å, c = 16.244 (5) Å, d_{obs} = 1.45, d_{calc} = 1.51 g cm^{-3}. The structure was refined to an R factor of 4.38, R_w = 5.16. The O–O atoms of the trigonal face are separated by 2.713 (3) Å, those related by the mirror plane by 2.526 (4) Å. The Fe–O distances are 2.012 (2) Å, and the bite angle is 77.75 (11)°. Solution thermodynamic studies on one of the ligands, bicappedTRENCAM, determine surprisingly low protonation constants (log K_1K_2 = 27.2 (1), log K_3 = 8.3 (1), log K_4K_5 = 8.73 (1), log $K_6K_7K_8$ = 9.75 (1)) containing a number of polyprotic steps. Aqueous electrochemical studies performed on the ferric complexes of these ligands show reversible reduction potentials of –0.89 to –0.97 V (vs NHE). While still highly selective for the ferric ion (ratios of the formation constants of ferric to ferrous complexes range from 28.1 to 29.5), these ligands have a slight stabilization of the ferrous complex relative to related tripodal compounds, one of which is the siderophore enterobactin. A slow protonation reaction is seen upon reduction of the ferric complexes. The protonation constant of the Fe(bicappedTRENCAM) complex proceeds in an unusual two-proton step with an equilibrium constant of (log K_1K_2) 10.65 (1). The complex formation constant (log K) is 43.1 (4), which shows no increase due to the macrobicyclic structure of the ligand relative to related hexadentate catechol ligands. The pM value is 30.7, where pM = –log [Fe] at pH 7.4 and $[Fe]_T = 10^{-6}$ M, $[L]_T = 10^{-5}$ M.

Introduction

The chemistry of metal ions in biological systems frequently shows remarkable specificity in complexing the targeted metal ion. The design of similar artificial sequestering agents, strongly and specifically to complex selected ions, has increasingly become an achievable goal. Thus, polyether and polyamine sequestering agents, with cyclic and bicyclic topologies, have produced metal complexes with unprecedented kinetic and thermodynamic stabilities.[2,3] Since nature has chosen the catechol ligand as the functional group in enterobactin, the siderophore which has the highest binding constant of these microbial iron binding agents,[4,5] we have selected catechol as the ligand to incorporate into a number of multidentate agents.[6,7] Introduction of the macrobicyclic framework into iron(III) sequestering agents was performed to see if similar increases in complexing ability could be achieved. The foremost feature of a macrobicyclic ligand is thermodynamic advantage, relative to less organized ligands.[8] Preorganizing the iron binding site should result in a higher formation constant. It should also produce a kinetically more stable complex[9] and result in markedly slower ligand exchange rates. In the limiting case it may be possible to produce an "inert" complex of high-spin Fe(III), a classic labile metal ion. Finally, the anticipated properties of these ligands suggest their potential use as pharmaceutical agents in ion decorporation or other sequestration applications.

In earlier catechol ligands we have incorporated 2,3-dihydroxyterephthalic acid, initially by using only one carboxylate group for attachment via an amide bond, with the remaining group used as a charged substituent to increase water solubility. More recently the research group of Vögtle[10,11] as well as we[12-14] have used both points of attachment of the 2,3-dihydroxyterephthalamide subunit (Figure 1) for macrocycle formation. We have recently shown that this subunit binds Fe(III) more strongly at physiological pH than any other bidentate chelate.[15] Thus it might

* To whom correspondence should be addressed.

(1) Paper no. 22 in the series Ferric Ion Sequestering Agents. For the previous paper in this series, see: Ng, C. Y.; Rodgers, S. J.; Raymond, K. N. *Inorg. Chem.* **1989**, *28*, 2062.
(2) Lehn, J.-M. *Science* **1985**, *227*, 849.
(3) Creaser, I. I.; Geue, R. J.; Harrowfield, J. MacB; Hertl, A. J.; Sargeson, A. M.; Snow, M. R.; Springborg, J. *J. Am. Chem. Soc.* **1982**, *104*, 6016. Geue, R. J.; Hambly, T. W.; Harrowfield, J. MacB.; Sargeson, A. M.; Snow, M. R. *J. Am. Chem. Soc.* **1984**, *106*, 5748.
(4) Matzanke, B. F.; Müller-Matzanke, G.; Raymond, K. N. *Iron Carriers and Iron Proteins*; Loehr, T. M., Ed.; Physical Bioinorganic Chemistry Series, VCH Publishers: New York, 1989; p 1.
(5) Raymond, K. N.; Müller, G.; Matzanke, B. F. *Top. Curr. Chem.* **1984**, *123*, 50.
(6) Raymond, K. N.; McMurry, T. J.; Garrett, T. M. *Pure Appl. Chem.* **1988**, *60*, 545.
(7) Raymond, K. N. *Environmental Inorganic Chemistry*; Irgolic, K. J., Martell, A. E., Eds.; VCH Publishers: Deerfield Beach, FL, 1985; p 331.
(8) Cram, D. J. *Angew. Chem., Int. Ed. Engl.* **1986**, *25*, 1039.
(9) Busch, D. H.; farmery, K.; Goedken, V.; Katovic, V.; Melnyk, A. C.; Sperati, C. R.; Tokel, N. *Advances in Chemistry Series*; Gould, R. F., Ed.; American Chemical Society: Washington, DC, 1971; Vol. 100, p 44.
(10) Kiggen, W.; Vögtle, F. *Angew. Chem., Int. Ed. Engl.* **1984**, *23*, 714.
(11) Stutte, P.; Kiggen, W.; Vögtle, F. *Tetrahedron* **1987**, *43*, 2065.
(12) Rodgers, S. J.; Ng, C. Y.; Raymond, K. N. *J. Am. Chem. Soc.* **1985**, *107*, 4094.
(13) McMurry, T. J.; Rodgers, S. J.; Raymond, K. N. *J. Am. Chem. Soc.* **1987**, *109*, 3451.
(14) McMurry, T. J.; Hosseini, M. W.; Garrett, T. M.; Hahn, F. E.; Reyes, Z. E.; Raymond, K. N. *J. Am. Chem. Soc.* **1987**, *109*, 7196.

0002-7863/91/1513-2965$02.50/0